buildings

MDPI

Article

Influence of Partial and Asymmetric Strengthening of Timber Floors on the Seismic and Gravity-Load Response of Historic Unreinforced Masonry Buildings

Ivan Volarić [1], Dean Čizmar [1,*], Mislav Stepinac [2] and Šime Serdarević [1]

[1] Department of Civil Engineering, Zagreb University of Applied Sciences, Avenija Većeslava Holjevca 15, 10000 Zagreb, Croatia; ivan.volaric@tvz.hr (I.V.)
[2] Faculty of Civil Engineering, University of Zagreb, Fra Andrije Kačića-Miošića 26, 10000 Zagreb, Croatia
* Correspondence: dean.cizmar@tvz.hr

Abstract

Historic unreinforced masonry (URM) buildings with flexible timber floors are seismically vulnerable because diaphragms deform in plane and wall–floor connections are often inadequate. In practice, strengthening may be limited to the attic or an asymmetric part of a storey. This study compares fourteen three-dimensional equivalent-frame models of two Zagreb URM building types through 336 nonlinear static analyses using the N2 method. A cross-laid 2 × 30 mm glued-laminated timber panel and an 80 mm timber–concrete composite slab were modelled at the attic only, at the attic and half of an intermediate floor, or at all levels above the basement. Separately, 144 joist cross-section/span combinations were assessed for ultimate and serviceability limit states under vertical actions. For TYPE A, attic-only strengthening increased the X-direction seismic resistance index (αSD) by 22.2% but reduced its Y-direction value by 27.3%. For TYPE B, comprehensive strengthening increased the minimum index by 40% (timber) and 32% (composite). Both vertical limit states were satisfied by 47.9%, 68.8%, and 84.7% of combinations for original, timber-strengthened, and composite-strengthened joists, respectively. For the analysed models, and assuming effective wall–floor connections, intervention continuity and distribution governed the global response more strongly than nominal diaphragm stiffness, while the resistance of the unstrengthened walls remained critical.

Keywords: historic masonry buildings; timber floor; partial strengthening; asymmetric strengthening; timber–concrete composite slab; N2 method; pushover analysis; seismic retrofit

Check for updates

Academic Editors: Sigong Zhang, Xiaoyue Zhang and Fei Tong

Received: 18 October 2026
Revised: 18 November 2026
Accepted: 23 November 2026
Published: 26 November 2026

Copyright: © 2026 by the authors. Licensee MDPI, Basel, Switzerland. This article is an open access article distributed under the terms and conditions of the Creative Commons Attribution (CC BY) license.

1. Introduction

Unreinforced masonry (URM) buildings with timber floors constitute a substantial part of the historic building stock of many European cities. In Zagreb, they are particularly characteristic of the Lower Town, which was built mainly from the late nineteenth century through the first decades of the twentieth century [1–3]. The load-bearing system typically consists of solid brick masonry walls in lime mortar, timber joists spanning between longitudinal walls, one or two layers of timber boarding, heavy rubble fill, and a plaster ceiling on reed lathing. Such floor structures have low in-plane stiffness and are commonly not reliably connected to the walls; consequently, reliable box-type behaviour may not develop during earthquakes.

The vulnerability of this typology was confirmed by the Zagreb earthquake of 22 March 2020 and the Petrinja earthquake of 29 December 2020 [4–7]. Observed dam-

age mechanisms included out-of-plane failure of gable and façade walls, separation of walls at intersections, damage to wall–floor connections, and shear failure of short masonry piers [5,8–11]. Strengthening the floors can reduce relative wall displacements and improve horizontal force transfer; however, an excessively stiff or spatially discontinuous diaphragm may simultaneously attract larger forces to critical masonry elements.

Previous studies, including recent numerical vulnerability assessments [12], show that the response of existing timber diaphragms lies between ideally flexible and fully rigid behaviour. In-plane stiffness depends on the orientation and continuity of timber boarding, fastener slip, openings, and connections to the walls [13–15]. Analytical and numerical procedures for explicitly accounting for floor deformability have also been developed for existing reinforced-concrete buildings, where in-plane floor flexibility was shown to affect both the structural response and the seismic fragility [16,17]. Strengthening systems include cross-planking [18,19], wood-based panels [20,21], steel or FRP strips [22–25], massive timber panels [21,26], and timber–concrete composite slabs [27–31]. Experimental evidence on the effect of diaphragm strengthening is available at the component level, from in-plane tests on original and retrofitted timber diaphragms [13,14,21,26] and tests on wall-to-floor connections [22,23], and at the building level, where shake-table tests on a full-scale unreinforced masonry building showed that stiffened floor and roof diaphragms combined with improved wall–diaphragm connections modified the global response and the activated damage mechanisms [32]. The present study is numerical and relies on this body of experimental work for the qualitative interpretation of the results. The stiffness of these systems can vary by orders of magnitude, while the global building response additionally depends on the continuity of strengthening in plan and over the building height.

In Croatian design practice, strengthening of existing masonry buildings is often carried out only partially, primarily in readily accessible zones such as the attic level or within only part of the floor plan. Such interventions may locally increase stiffness and strength substantially, while at the same time changing the distribution of mass, stiffness, and seismic forces and introducing or increasing plan and vertical irregularities that are not always assessed systematically after intervention.

The Croatian Reconstruction Act [33] and the Technical Regulation for Building Structures [34] establish the legal and technical framework for post-earthquake rehabilitation. The Technical Regulation defines target values of the significant-damage index (IZO) of at least 0.50, 0.75, and 1.00 for the corresponding levels of structural rehabilitation. This graded approach is justified by the need to balance safety, cost, and heritage-conservation requirements; however, in design practice it may also encourage optimisation of interventions toward satisfying the minimum prescribed threshold rather than achieving balanced and mechanically consistent behaviour of the structure as a whole. This issue is particularly relevant to Level 2 rehabilitation (IZO ≥ 0.50), for which an isolated numerical index does not, by itself, demonstrate adequate local failure prevention or reliable wall–floor anchorage.

An additional issue is that assessment of existing masonry buildings in practice is often based on equivalent-frame software and nonlinear static analysis. Such models are highly efficient for engineering applications, but they rely on simplified assumptions and prescribed diaphragm behaviour. It is also important to emphasise that strengthening a floor does not automatically improve its behaviour under vertical actions. Historic timber floors are often characterised by low flexural stiffness, long-term creep deformation, material degradation, and uncertain connection conditions; consequently, serviceability may remain governing even when the strengthened diaphragm becomes more effective seismically.

The aim of this study is to quantify the influence of the extent and type of strengthening on two representative types of historic URM buildings. The investigation combines: (i) 14 three-dimensional models assessed using nonlinear static analysis and the N2 method; (ii)

comparison of the original condition, attic-only strengthening, plan-asymmetric partial strengthening, and comprehensive strengthening of all levels above the basement; (iii) comparison of a cross-laid 2 × 30 mm glued-laminated timber panel and a timber–concrete composite slab with an 80 mm reinforced-concrete layer; and (iv) a parametric verification of the strength and serviceability of existing and strengthened timber joists.

The study is based on the authors' numerical models with systematically varied parameters. Its main contribution is an integrated interpretation of floor strengthening under horizontal and vertical actions, with particular emphasis on partial and asymmetric interventions, which are common in the rehabilitation of historic URM buildings but remain insufficiently addressed in the available literature.

2. Review of Previous Research

2.1. Floor Stiffness and Global Seismic Response

A rigid diaphragm distributes inertial forces according to the stiffness of the vertical elements, whereas in a flexible diaphragm internal shear and flexural deformations may be comparable to wall displacements, so that walls act partly independently.

Wilson et al. [13] demonstrated the orthotropic behaviour of existing timber diaphragms, while Brignola et al. [14] quantified the influence of board arrangement and fasteners. Numerical analyses by Tomić et al. [15] showed that assuming a rigid diaphragm when the actual floor is flexible can substantially overestimate building capacity. Conversely, rigid coupling without adequate wall and connection capacity can concentrate forces in vulnerable masonry piers and spandrels. Idealised components of the in-plane floor response are shown in Figure 1.

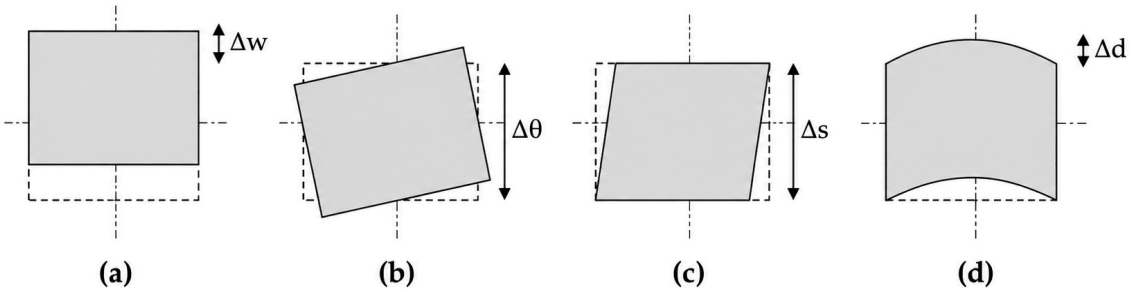


Figure 1. Idealised components of the in-plane floor response: (**a**) translation; (**b**) rotation; (**c**) shear deformation; (**d**) flexural deformation. Authors' illustration.

2.2. Strengthening Systems for Timber Floors

Experimental studies have identified a wide hierarchy of system stiffness. A single layer of traditional timber boarding generally remains highly flexible. A second layer of boards placed perpendicular to the first can substantially increase stiffness, while diagonal steel or FRP strips provide directional tensile force transfer but depend strongly on anchorage [22–25]. Continuous timber panels and timber–concrete composite slabs provide the greatest increases in stiffness; however, the timber–concrete solution introduces a wet construction process, greater mass, and more efficient force transfer to the existing masonry [21,26–31].

Timber-based solutions are advantageous for historic URM buildings because of their low mass, material compatibility, and potential reversibility. Timber–concrete composite (TCC) systems use timber predominantly in tension and concrete in compression, achieving high flexural stiffness and effective diaphragm action [27–31]. In both cases, behaviour depends on connection slip, while the global contribution may be limited by the capacity of the existing walls and supports.

The idealised intervention extents analysed in this study are shown in Figure 2. Such attic-only and spatially partial interventions reflect practical constraints encountered during the post-earthquake rehabilitation of historic URM buildings in Zagreb. Level 2 rehabilitation requires an IZO of at least 0.50 under the applicable Croatian technical framework [34].



Figure 2. Idealised intervention extents analysed for TYPE A and TYPE B: (**a**) original condition; (**b**) attic-level strengthening only; (**c**) strengthening of the attic and one half of the floor above the first storey; (**d**) strengthening of all levels above the basement. TYPE A comprises a basement, ground floor, and three upper storeys, whereas TYPE B comprises a basement, ground floor, and two upper storeys.

Street-façade photographs of the analysed buildings are shown in Figure 3: the TYPE A building is shown on the left and the TYPE B building on the right.



Figure 3. Street façades of the analysed historic buildings in Zagreb: TYPE A on the left and TYPE B on the right. Authors' photographs.

2.3. Mechanical Properties of Existing Timber and Masonry

The mechanical properties of existing timber cannot be taken directly from strength classes intended for new sawn timber. Investigations of historic Croatian and other European timber structures have shown pronounced heterogeneity associated with moisture, knots, biological degradation, and local loss of cross-section [35–40]. A conservative reference class C20 according to EN 338 [41] was therefore adopted for the parametric analysis, with the explicit limitation that this assumption does not replace inspection and testing of a specific building.

The properties of historic masonry in Zagreb also show considerable scatter. Flat-jack and sonic testing have yielded elastic-modulus and shear-strength values both above and below commonly used reference values [42–46]. In this study, conservative but realistic properties were adopted for solid-brick masonry in lime mortar and kept identical for all strengthening variants.

3. Materials and Methods

3.1. Typological Models

Two representative types of historic residential buildings were selected. Both types represent recurring configurations of the residential building stock of the Zagreb Lower Town built between the late nineteenth century and the first decades of the twentieth century: TYPE A corresponds to a street-facing block with a central staircase, and TYPE B to a block with courtyard wings and short courtyard walls. In both, timber floors span between the longitudinal walls and the basement is covered by shallow brick vaults spanning between steel beams (jack arches), which is the prevailing structural arrangement of this stock [1–3]. The two types do not cover the full typological variability (e.g., corner buildings, buildings with steel-beam or reinforced-concrete floors, or buildings altered by later additions); the results should therefore be interpreted as indicative of these two configurations rather than of the building stock as a whole. TYPE A has an elongated street-facing wing with a staircase zone located approximately at the centre of the plan, whereas TYPE B includes courtyard wings, recessed portions, and short longitudinal walls in the courtyard zone. Geometry was taken from the final 3Muri models, and the numerical dimensions in Table 1 were determined from the coordinates of the outermost model nodes. TYPE A has one additional storey level, whereas TYPE B, despite its lower height, contains more three-dimensional nodes because of its more complex plan arrangement. The floor plans and three-dimensional models of both types are shown in Figure 4. In the 3Muri models, the floors above the basement were defined as steel-beam-and-vault floors (vault span 1.30 m, rise 0.20 m, vault thickness 0.14 m), and all walls are fixed at the foundation level.

In both models, the walls were discretised according to the actual load-bearing masonry lines and openings. Wall thickness decreases toward the upper storeys. TYPE A basement walls are 45–75 cm thick and the above-ground walls are 30–60 cm thick. For TYPE B, basement walls are 20–80 cm thick, and the above-ground walls are predominantly 20–60 cm thick. These differences, together with the locations of the staircase and courtyard wings, produce different torsional sensitivities and different critical wall mechanisms.

Table 1. Basic geometric and discretisation data of the numerical models.

Parameter	TYPE A	TYPE B
Model plan dimensions X × Y	22.55 × 12.30 m	12.85 × 18.05 m
Modelled storey levels	basement + ground floor + 3 upper storeys	basement + ground floor + 2 upper storeys
Characteristic storey heights	3.00 m basement; 3.65 m above ground	3.80 m all storeys
Range of basement wall thicknesses	45–75 cm	20–80 cm
Range of above-ground wall thicknesses	30–60 cm	20–60 cm
Number of wall lines in the model	26	19
Number of unique 3D nodes	150	172
Pushover control node	node 142, Level 5	node 90, Level 4

Note: Plan dimensions represent approximate external model dimensions obtained from the coordinates of the outermost nodes and exclude roof overhangs. The attic diaphragm is located at the highest modelled storey level (TYPE A—Level 5 at elevation 17.60 m; TYPE B—Level 4 at elevation 15.20 m), where the pushover control node is also located.

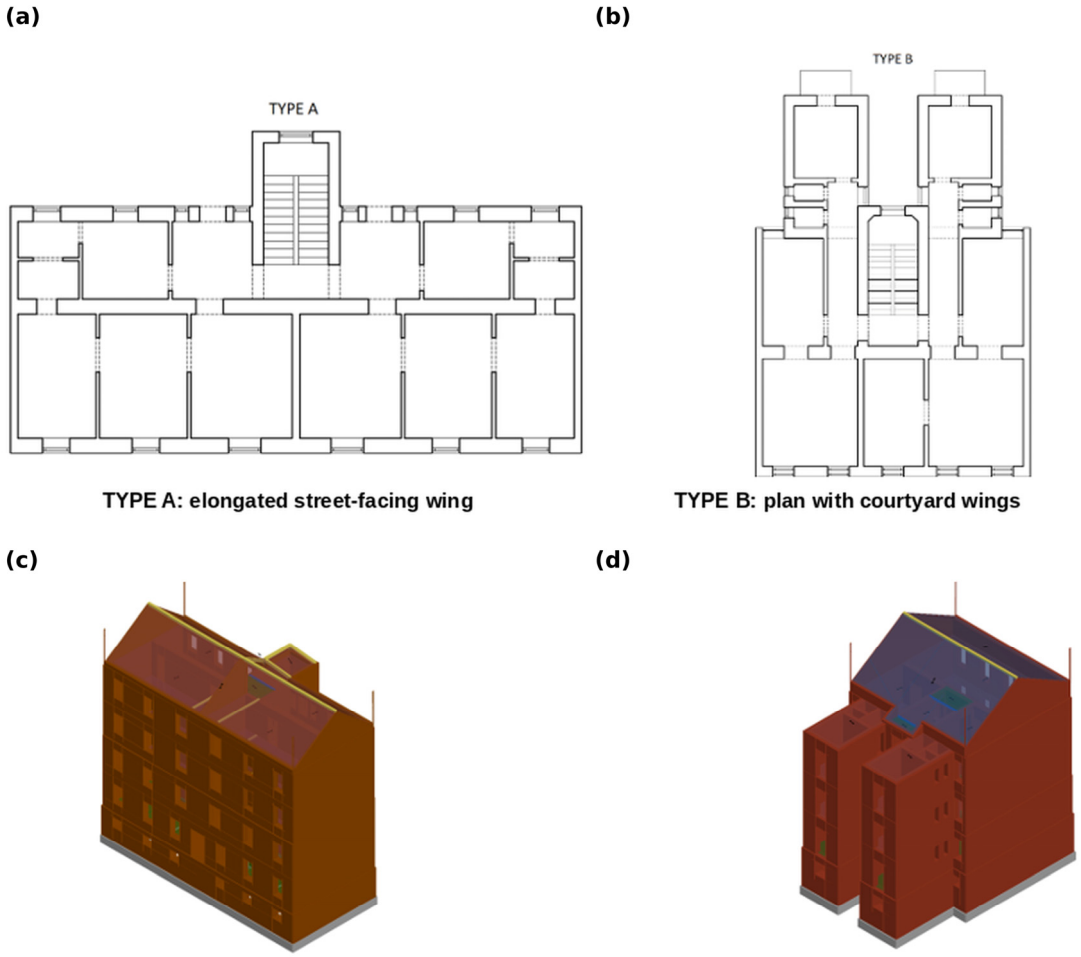


Figure 4. Analysed typological models: (**a**) plan of TYPE A; (**b**) plan of TYPE B; (**c**) three-dimensional model of TYPE A; (**d**) three-dimensional model of TYPE B. Model views generated in 3Muri.

3.2. Strengthening Variants

Seven configurations were analysed for each building type: the original condition and six strengthened variants obtained by combining two strengthening systems with three intervention extents. The timber system consists of a timber panel of two cross-laid 30 mm GL24h glued-laminated timber layers (2 × 30 mm) in accordance with EN 14080 [47], whereas the timber–concrete system consists of a composite slab with an 80 mm C25/30 concrete layer and B500B reinforcement. The walls were not strengthened in any variant. All analysed configurations and their designations are summarised in Table 2.

Table 2. Analysed strengthening configurations.

Designation	System	Intervention Extent	Plan Regularity	Vertical Continuity
I	Original timber floor	No intervention	Original condition	Original condition
D-T	Timber panel 2 × 30 mm	Attic only	Symmetric at attic	Discontinuous
D-P	Timber panel 2 × 30 mm	Attic + left half of floor above first storey	Asymmetric	Discontinuous
D-S	Timber panel 2 × 30 mm	All levels above basement	Predominantly symmetric	Continuous above basement
TC-T	Composite slab 80 mm	Attic only	Symmetric at attic	Discontinuous
TC-P	Composite slab 80 mm	Attic + left half of floor above first storey	Asymmetric	Discontinuous
TC-S	Composite slab 80 mm	All levels above basement	Predominantly symmetric	Continuous above basement

In the partial variants, in addition to strengthening the attic level, one half of the floor above the first storey was strengthened on the negative side of the global X-axis (the left half of the plan in Figure 4a). For the timber variant, the rubble fill is removed at the attic level, and the panel is installed from above; at residential levels, the fill is retained, the ceiling layers are removed, and the panel is installed from below. For the composite slab, the rubble fill is removed in all strengthened zones. The "all levels" variant does not include the floor above the basement.

3.3. Mechanical Properties of Masonry and Nonlinear Constitutive Law

The same set of masonry mechanical properties was applied to all 14 models (Table 3). The modulus of elasticity E = 1500 N/mm^2 is very close to the value of 1469.5 N/mm^2 measured at the Prince Rudolf Infantry Barracks complex in Zagreb, a building of comparable age and structural system [46]. The reference shear strength $\tau 0$ = 0.15 N/mm^2 was selected conservatively so that favourable local test results would not be uncritically assigned to the entire historic building stock. The same source reports a measured initial shear strength fv0 = 0.323 N/mm^2 and a friction coefficient μ = 0.447 for that building [46]; the adopted $\tau 0$ = 0.15 N/mm^2 is therefore less than half of the locally measured value, quantitatively supporting the conservative selection.

In the automatic 3Muri reports, the mean compressive strength and reference shear strength are reported as 2.96 N/mm^2 and 0.11 N/mm^2. Numerically, these values correspond to the reference values of 4.00 N/mm^2 and 0.15 N/mm^2 divided by the confidence factor CF = 1.35. The material partial factor γ_M = 2.00 is stated separately and is not applied again to the reported effective values. Table 3 therefore distinguishes between reference material properties, the confidence factor, the partial factor, and the values reported by the software.

Table 3. Mechanical properties of masonry used in the numerical models.

Property	Symbol	Reference Value	Value in Report	Unit
Modulus of elasticity	E	1500	1500	N/mm^2
Shear modulus	G	500	500	N/mm^2
Mass density	ρ	1835	1835	kg/m^3
Mean compressive strength	f_m	4.00	2.96 *	N/mm^2
Characteristic compressive strength	f_k	3.00	—	N/mm^2
Reference shear strength	τ_0	0.15	0.11 *	N/mm^2
Limiting shear strength	$f_{v,lim}$	0.65	0.65	N/mm^2
Material partial factor	γ_M	2.00	—	—
Confidence factor	CF	1.35	—	—

* Values in the automatic report correspond to the reference values reduced by the confidence factor CF = 1.35.

The adopted elastic and shear moduli, E = 1500 N/mm^2 and G = 500 N/mm^2, are the central values of the ranges recommended for solid-brick masonry in lime mortar in the Italian code commentary (E = 1200–1800 N/mm^2, G = 400–600 N/mm^2) [48], and E = 1500 N/mm^2 also lies close to the centre of the large scatter of the elastic moduli measured by flat-jack tests on historic brick masonry in Croatia [45]. The effective strengths used in the analyses after division by CF = 1.35 (f_m = 2.96 N/mm^2, τ0 = 0.11 N/mm^2) lie within the corresponding ranges of [48] (f_m = 2.6–4.3 N/mm^2, τ0 = 0.05–0.13 N/mm^2). The adopted properties therefore represent central rather than bounding values. Because they were kept identical in all seven configurations of each building type, an uncertainty in their absolute values affects all configurations of a type in the same direction; the study therefore addresses the relative influence of floor strengthening, and the absolute αSD values are conditional on the adopted material parameters (Sections 5.5 and 5.6).

The initial masonry stiffness was defined as cracked. Nonlinear macroelement behaviour was represented by a bilinear law, with nonlinearity activated when the lower of the shear or flexural resistance was reached. In the plastic range, stiffness degradation occurs, and deformation capacity is limited by the maximum permissible interstorey drift, depending on the damage mechanism. Once the limit conditions are reached, the element is removed from the load-bearing system without automatic termination of the global analysis.

3.4. Modelling of Floor Structures, Loads, and Mass

Horizontal structures were modelled using three-node surface elements connected to the three-dimensional wall nodes. The elements have in-plane stiffness but no out-of-plane flexural stiffness because membrane transfer of horizontal forces is governing in the global seismic model. The original timber floor was modelled as a one-way orthotropic element with E_x = 9500 N/mm^2, E_y = 0, and a very low shear modulus G = 10 N/mm^2. The strengthened variants have finite two-way stiffness. An effective connection of the structural panel to the existing joists and walls was assumed, without explicit modelling of anchor slip or local separation. Most of the difference between variants results from the membrane shear stiffness G_t. Relative to the original timber element, the timber panel has approximately 108 times greater G_t, while the timber–concrete composite slab has approximately 2583 times greater G_t. At the same time, the longitudinal membrane stiffness E_{xt} is approximately 2.83 times greater for the timber panel and 7.53 times greater for the composite slab. The ratios refer to the equivalent membrane values in Table 4 and were

not derived from the characteristic material properties presented in Section 3.6. In the global model, the cross-laid 2 × 30 mm timber panel was entered using the 3Muri floor type with two overlapping, mutually orthogonal plank layers (2 × 30 mm, GL24h) on C20 joists (b × h = 160 × 200 mm at 800 mm). For this floor type, the software smears the plank layers over the total thickness and assigns them the mean modulus of elasticity parallel to the grain of the selected planking material in both directions (GL24h, 11,600 N/mm^2 in the software library), while the joists contribute only to E_x (E_{C20}·b·h/(i·t) = 6333 N/mm^2, giving E_x = 17,933 N/mm^2). The value E_y = 11,600 N/mm^2 in Table 4 is therefore not a modulus perpendicular to the grain. The in-plane response of the strengthened timber diaphragm is governed mainly by the membrane shear modulus G = 720 N/mm^2.

Table 4. Numerical properties of floor elements and area loads in the global 3Muri models.

System/Zone	t (mm)	G (N/mm^2)	E_x (N/mm^2)	E_y (N/mm^2)	ν	G_{k1} (kN/m^2)	G_{k2} (kN/m^2)	Q_k (kN/m^2)
Vaults above basement	40	400	11,501.54	0	—	3.86	3.45	2.00
Original timber floor—standard storeys	40	10	9500	0	—	0.16	3.79	2.00
Original timber floor—attic	40	10	9500	0	—	0.16	2.48	2.00
Timber panel 2 × 30 mm—attic, rubble fill removed	60	720	17,933.33	11,600	—	0.42	0.32	2.00
Timber panel 2 × 30 mm—residential storeys, rubble fill retained	60	720	17,933.33	11,600	—	0.42	3.67	2.00
Timber–concrete composite slab 80 mm—strengthened zones	80	12,916.67	35,750	31,000	0.20	2.25	0.32	2.00

The self-weight of volumetric elements was generated automatically from geometry and material density, whereas additional permanent layers were entered as G_{k2}. For standard timber floors, the detailed sum of layers is 3.79 kN/m^2; for the attic floor, 2.48 kN/m^2; for the vaults above the basement, 3.45 kN/m^2; and for the roof, 0.946 kN/m^2. The imposed load on residential floors is 2.00 kN/m^2. Snow and wind were not combined with the seismic design situation. The total seismic mass of each model, obtained from the modal analysis, changed relative to the original condition by −2.0%, −1.9%, and −1.6% for the timber variants and by −0.1%, −0.7%, and −4.1% for the composite variants of TYPE A (T, P, and S, respectively), and by −1.9%, −1.9%, −1.8% and −0.1%, −1.1%, −2.9% for TYPE B. In the attic-only composite variants (TC-T), the removed rubble fill is almost exactly compensated by the concrete layer (G_{k1} + G_{k2} = 2.57 kN/m^2 compared with 2.64 kN/m^2 for the original attic floor, Table 4).

3.5. Equivalent-Frame Model, Seismic Demand, and the N2 Method

The three-dimensional numerical models and all modal, static, and nonlinear static analyses were carried out in 3Muri version 14.2.0.4 (x64), Professional edition (S.T.A. DATA S.r.l., Turin, Italy) [49], using the Modal Analysis, Static Analysis, and Pushover Analysis modules. The models were developed using the equivalent-frame approach. Masonry piers and spandrels were represented by deformable nonlinear macroelements, whereas less damage-prone masonry zones were represented by rigid nodes [49–52]. Three-dimensional nodes have three translational degrees of freedom and rotations about the X and Y axes, enabling force transfer between mutually perpendicular walls; two-dimensional nodes are used within the plane of an individual wall.

The seismic demand was defined for Zagreb. A reference peak ground acceleration a_{gR} = 0.256 g was adopted for a return period of 475 years, and a_{gR} = 0.129 g for a return period of 95 years. The buildings belong to importance class II with γI = 1.00. For ground type C, the parameters S = 1.15, TB = 0.20 s, TC = 0.60 s, and TD = 2.00 s were used. All αSD results shown in the principal comparison refer to the Significant Damage limit state and the corresponding demand for a return period of 475 years.

For each model, 24 pushover analyses were performed by combining four loading directions (+X, −X, +Y, and −Y), two horizontal force distributions, and accidental eccentricity. The first distribution was uniform and proportional to mass, whereas the second was proportional to the product of mass and the deformation shape of the dominant mode. Eight analyses were performed without eccentricity and sixteen with ±5% of the plan dimension perpendicular to the loading direction. The settings were identical for all 14 models and were consistent with the principles of the N2 method and Eurocode 8 [34,53–55]. A total of 336 nonlinear static analyses were therefore performed (14 models × 24 analyses). The seismic demand and analysis settings are summarised in Table 5.

Table 5. Seismic demand and settings of the nonlinear static analyses.

Parameter	TYPE A	TYPE B	Note
Location	Zagreb	Zagreb	—
Reference acceleration, TR = 475 years	0.256 g	0.256 g	Significant Damage limit state
Reference acceleration, TR = 95 years	0.129 g	0.129 g	additional reference spectrum
Importance class/γI	II/1.00	II/1.00	—
Ground type/S/TB/TC/TD	C/1.15/0.20/0.60/2.00 s	C/1.15/0.20/0.60/2.00 s	—
Number of pushover analyses per model	24	24	4 directions × 2 distributions × eccentricities
Accidental eccentricity for X loading	0; ±61.50 cm	0; ±90.25 cm	5% of Y dimension
Accidental eccentricity for Y loading	0; ±112.75 cm	0; ±64.25 cm	5% of X dimension
Control node	node 142, Level 5	node 90, Level 4	highest regular storey level
Initial masonry stiffness	cracked	cracked	same in modal and nonlinear analyses

The seismic resistance index is defined as the ratio of acceleration capacity to acceleration demand for the Significant Damage limit state:

$$\alpha SD = PGAC,SD/PGAD,SD$$

A value of αSD = 1.00 indicates that the capacity equals the required seismic acceleration, whereas a value below 1.00 represents the fraction of the demand that the model can sustain. In the Technical Regulation [34], this ratio corresponds to the significant-damage index IZO; the notation αSD is used throughout this paper. The displacement check is based on $d_{t,SD} \leq d_{m,SD}$, where $d_{t,SD}$ is the required target displacement and $d_{m,SD}$ is the available global displacement capacity obtained from the bilinearised capacity curve [34,53–55].

Pushover analyses were terminated when the base shear dropped by 20% relative to its peak value. When an important wall element entered the Significant Damage state and

further redistribution was judged to be mechanically unjustified or likely to compromise the vertical load-bearing capacity of the wall supporting the floors, the capacity curve was manually truncated at that analysis step. The criterion was applied consistently to all variants and strengthening types. Because this decision involves engineering judgement regarding the reliability of the vertical load path, its influence is specifically addressed in the study limitations. Quantitatively, a capacity curve was truncated at the analysis step at which a pier of a load-bearing wall supporting the floors reached incipient shear failure, shear failure, or the "ineffective element" state of the damage classification of the software, i.e., when its capacity to carry vertical load could no longer be relied upon. In all 28 governing analyses (14 models × 2 directions), this criterion was reached before a 20% drop in the base shear, so that the dm values correspond to the truncation criterion. The governing analysis, the wall in which the criterion was reached, the truncation step relative to the total number of analysis steps, and the resulting dm are listed for all models in Appendix A (Table A1).

3.6. Parametric Analysis Under Vertical Actions

The parametric verification under vertical actions was performed using a separate model of a characteristic timber joist and was not taken directly from the global 3Muri model. A floor with a total depth of approximately 390 mm and joists spaced at 0.90 m centres was analysed (Figure 5). In this model, the additional permanent load from floor layers, fill, ceiling, services, joists, and an equivalent load representing partition walls was 3.36 kN/m^2, while the imposed load was 2.0 kN/m^2. The difference from the area loads used in the global model results from the different level of idealisation and the separate treatment of self-weight.

Spans from 3.5 to 6.0 m were combined with joist widths from 140 to 240 mm and depths of 200, 220, 240, and 280 mm, yielding 144 combinations for each system. Ultimate limit state (ULS) and serviceability limit state (SLS) checks were performed according to Eurocode 5 [56]. The existing joists were assigned strength class C20, with characteristic material values adopted in accordance with EN 338 [41] and the properties listed in Table 6, while actions were determined according to EN 1991-1-1 [57]. Variants with a cross-laid 2 × 30 mm GL24h timber panel and a timber–concrete composite slab with an 80 mm concrete layer were compared. The SLS check was performed for the instantaneous deflection under the characteristic load combination, $w_{inst} \leq L/300$; long-term deflection due to creep was not included in the reported counts and is discussed in Sections 5.4 and 5.6. For the timber panel, only the 30 mm layer with the grain parallel to the joists was taken as the compression flange of a T-section with an effective width equal to the joist spacing (900 mm), while the cross layer was applied as an additional permanent load (0.10 kN/m); composite action with the joists was calculated by the γ-method (EN 1995-1-1, Annex B [56]) with self-tapping screws Ø8 × 155 mm at 100 mm spacing in two rows (equivalent single-row spacing 50 mm), a slip modulus K_{ser} = 2085 N/mm per screw (EN 1995-1-1, Table 7.1, with ρ_k = 330 kg/m^3), $K_u = 2K_{ser}/3$. The ULS was verified at t = 0 (E_{mean}, K_u) and at t = ∞ ($E_{mean}/(1 + kdef)$ and $K_u/(1 + 2kdef)$, i.e., with kdef doubled for the connection [56]) for combined bending and tension of the joist, combined bending and compression of the flange, shear of the joist (k_{cr} = 0.67), and the shear resistance of the screws (R_k = 4.77 kN per screw); the instantaneous deflection was calculated with K_{ser}, and the final deflection with $E_{mean}/(1 + kdef)$ and $K_{ser}/(1 + 2kdef)$ for permanent load and the corresponding values with $\psi 2$ = 0.3 for imposed load. The timber–concrete composite slab was calculated with MyProject, version 5.50, CTC module (Rotho Blaas S.r.l., Cortaccia, Italy) using CTC 7 × 240 mm concrete-to-timber screws (ETA-19/0244) installed as crossed pairs at 45° in two rows, with spacing varying from 100 mm near the supports to 200 mm at midspan

(effective spacing 125 mm), K_{ser} = 10,825 N/mm at t = 0 and 6766 N/mm at t = ∞, and the joists propped during casting. Both calculations include the connector shear verification at t = 0 and t = ∞. For the representative 200 × 240 mm joist with a 5.0 m span, the connector utilisation is 65% (t = 0) and 54% (t = ∞) for the timber panel and 53% (t = 0) and 56% (t = ∞) for the composite slab, and the final deflections are 18.0 mm (L/278) and 9.5 mm (L/524), respectively.

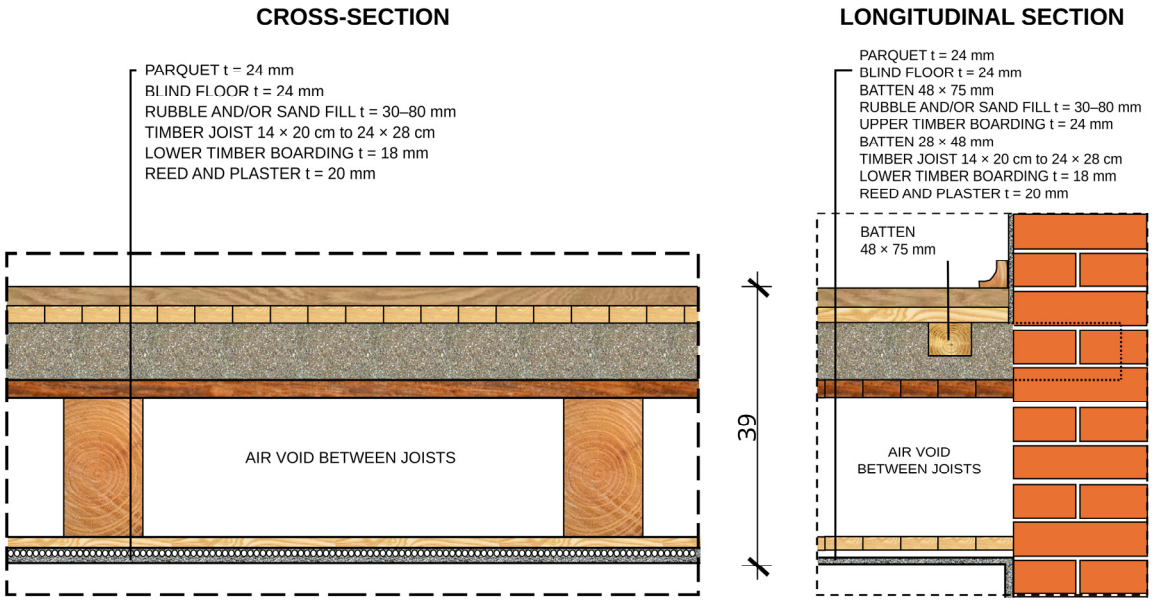


Figure 5. Characteristic cross-section and longitudinal section of the original timber floor, with a total depth of approximately 390 mm. Illustration based on the characteristic historic timber-floor construction described in [3]; drawn by the authors.

Table 6 presents timber-based materials commonly used in Croatia for structural rehabilitation and strengthening of timber floors. Particular attention is given to OSB/3 panels, which are widely used but, based on the comparison of mechanical properties, are not an optimal choice for increasing vertical load-bearing capacity and stiffness. Their modulus of elasticity is approximately 52% of the C20 value, while kdef = 1.50 is 2.5 times the value for solid and glued-laminated timber [41,58]. The consequence is lower effective flexural stiffness and greater long-term deflection.

Table 6. Mechanical properties of materials considered in the selection of strengthening systems.

Material	Characteristic Density ρ_k (kg/m³)	E (N/mm²)	E/E_{ref}	$f_{m,k}$ (N/mm²)	k_{mod}	k_{def}
Solid timber C20	330	9500	1.00	20	0.80	0.60
Glued-laminated timber GL24h	385	11,500	1.21	24	0.80	0.60
Plywood	600	5500	0.58	36	0.80	0.80
LVL	520	13,800	1.45	44	0.80	0.60
OSB/3	600	4930	0.52	14.8 (t = 18–25 mm)	0.70	1.50

4. Results

4.1. Modal Response and Participating Mass

In the original TYPE A model, the response is distributed among a larger number of modes. The first dominant mode in the Y direction has a period of 0.699 s and activates 43.79% of the mass, while the dominant response in the X direction appears only in the sixth mode, with a period of 0.399 s and a participating mass of 43.22%. After strengthening, the response becomes more concentrated: the first Y-dominant mode activates approximately 68% of the mass, the dominant response in the X direction shifts to the third mode, and the total participating mass in the X direction increases from 67.73% to 81.9–83.4%.

The original TYPE B model already exhibits more clearly separated translational modes. The first mode acts predominantly in the X direction, with a period of 0.553 s and a participating mass of 61.31%. After strengthening, the dominant period in the X direction decreases to 0.497–0.515 s. The total participating mass in the X direction increases from 70.88% to 76.20–84.78%, while in the Y direction it generally increases from 82.60% to 84.51–93.19%. The partial composite-slab variant is an exception, with 82.33% participating mass in the Y direction, confirming that a local increase in stiffness does not necessarily improve the global modal response.

The dominant modes of the original models are presented in Table 7. TYPE A exhibits a more distributed response, with the Y direction dominant in the early modes and the X direction becoming dominant only in the sixth mode, whereas TYPE B shows more clearly separated translational modes. The total participating modal masses of all configurations are shown in Figure 6 for TYPE A and Figure 7 for TYPE B.

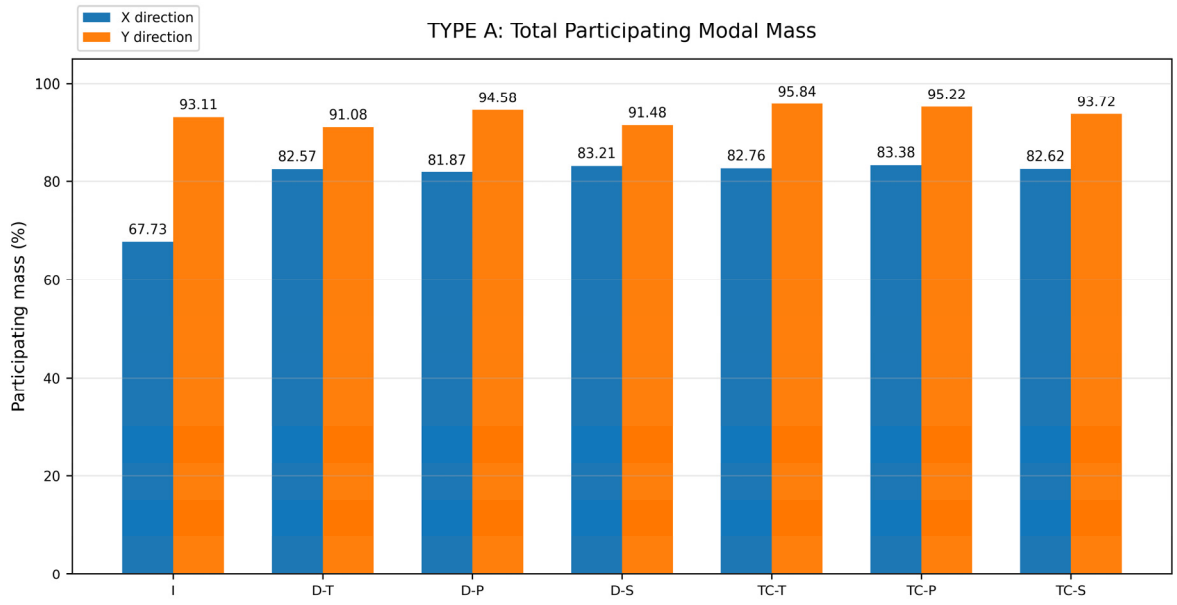


Figure 6. Total participating modal mass for TYPE A in the original and strengthened conditions. I—original; D—timber panel; TC—timber–concrete composite slab with a reinforced-concrete compression layer; T—attic; P—partial; S—all levels above the basement.

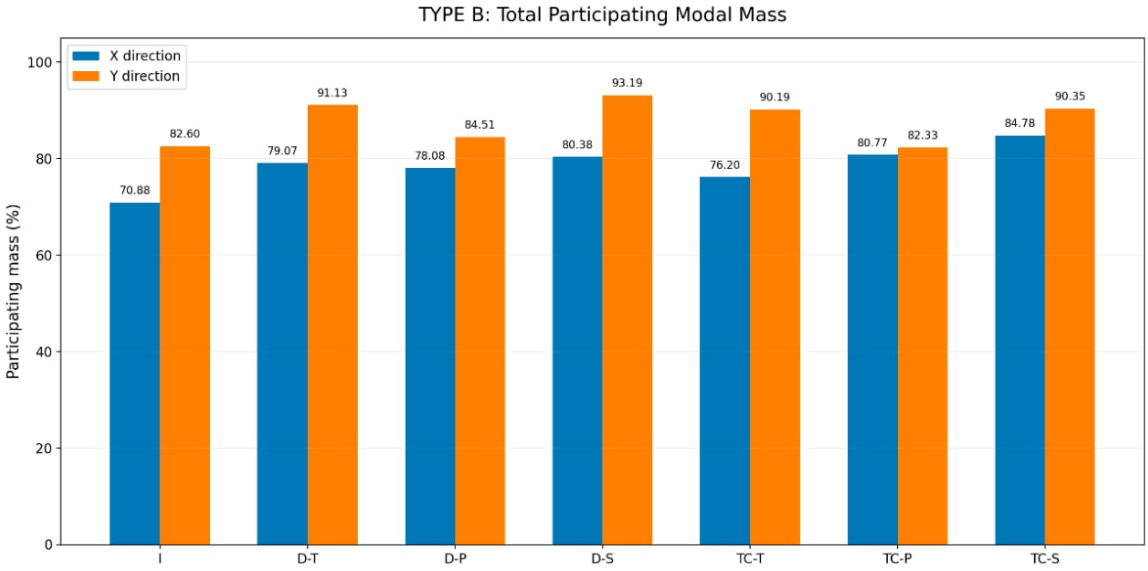


Figure 7. Total participating modal mass for TYPE B in the original and strengthened conditions. Variant designations are the same as in Figure 6.

Table 7. Dominant modal shapes of the original models.

Type	Mode	T (s)	Mx (%)	My (%)	Response Character
TYPE A	1	0.699	0.00	43.79	Y-dominant
TYPE A	4	0.548	0.00	24.04	additional Y
TYPE A	6	0.399	43.22	0.00	X-dominant
TYPE A	7	0.332	17.20	0.00	additional X
TYPE B	1	0.553	61.31	0.00	X-dominant
TYPE B	7	0.334	0.00	73.15	Y-dominant
TYPE B	10	0.195	9.58	0.00	additional X
TYPE B	16	0.142	0.00	9.54	additional Y

4.2. Seismic Resistance Index and Displacement Capacity

Table 8 presents αSD, available displacement capacity, and participating-mass values for all analysed configurations.

For TYPE A, strengthening only the attic level increases αSD,X from 0.36 to 0.44 (+22.2%) but reduces αSD,Y from 0.33 to 0.24 (−27.3%). Adding partial strengthening of one half of the floor above the first storey increases αSD,Y only to 0.25, while αSD,X decreases to 0.42. The intervention is therefore more extensive but not more effective. Comprehensive strengthening of all levels above the basement produces a more balanced response: the timber panel yields 0.43 in the X direction and 0.32 in the Y direction, while the timber–concrete composite slab yields 0.42 and 0.32. The minimum directional index remains slightly below the original value. Thus, for TYPE A, none of the six analysed variants increased the governing (minimum directional) αSD relative to the original condition.

For TYPE B, attic-only strengthening produces a moderate improvement. Comprehensive strengthening is clearly the most effective: the timber panel increases αSD from 0.25 to 0.35 in the X direction and from 0.35 to 0.43 in the Y direction, while the timber–concrete composite slab yields 0.33 and 0.44. The minimum directional index increases by 40% for the timber variant and by 32% for the composite variant.

Table 8. Summary of N2-method results for all configurations.

Type	Configuration	αSD,X	αSD,Y	min. αSD	dm,X (mm)	dm,Y (mm)	Mx (%)	My (%)
TYPE A	Original condition	0.36	0.33	0.33	45.00	61.30	67.73	93.11
TYPE A	Timber panel—attic	0.44	0.24	0.24	69.97	38.31	82.57	91.08
TYPE A	Timber panel—partial	0.42	0.25	0.25	65.02	39.76	81.87	94.58
TYPE A	Timber panel—all above basement	0.43	0.32	0.32	53.98	50.31	83.21	91.48
TYPE A	Timber–concrete composite slab—attic	0.44	0.24	0.24	71.03	38.85	82.76	95.84
TYPE A	Timber–concrete composite slab—partial	0.42	0.25	0.25	66.01	38.80	83.38	95.22
TYPE A	Timber–concrete composite slab—all above basement	0.42	0.32	0.32	53.02	47.75	82.62	93.72
TYPE B	Original condition	0.25	0.35	0.25	40.74	22.45	70.88	82.60
TYPE B	Timber panel—attic	0.30	0.37	0.30	44.07	22.44	79.07	91.13
TYPE B	Timber panel—partial	0.27	0.37	0.27	43.13	22.44	78.08	84.51
TYPE B	Timber panel—all above basement	0.35	0.43	0.35	51.28	26.36	80.38	93.19
TYPE B	Timber–concrete composite slab—attic	0.29	0.35	0.29	43.28	22.44	76.20	90.19
TYPE B	Timber–concrete composite slab—partial	0.27	0.36	0.27	42.33	22.44	80.77	82.33
TYPE B	Timber–concrete composite slab—all above basement	0.33	0.44	0.33	51.12	27.16	84.78	90.35

For TYPE A, the available displacement capacities dm in the attic-only and partial variants become strongly direction-dependent: dm,X increases from 45.0 mm to approximately 65–71 mm, while dm,Y decreases from 61.3 mm to approximately 38–40 mm. Comprehensive strengthening reduces this difference. For TYPE B, comprehensive strengthening simultaneously increases the available displacement capacity dm and αSD, indicating greater global deformation capacity before the governing limit state is reached.

The governing values for the original condition are associated with analyses that include the modal force distribution and accidental eccentricity (Table 9). This confirms that plan torsional sensitivity affects the minimum directional result of both models. Directional αSD values are shown in Figure 8 for TYPE A and Figure 9 for TYPE B, while relative changes with respect to the original condition are given in Table 10.

Table 9. Governing pushover analyses of the original models according to the minimum αSD.

Type	Direction	Analysis	Sign	Distribution	e (cm)	αSD
TYPE A	X	16	−X	modal	−61.50	0.360
TYPE A	Y	19	+Y	modal	+112.75	0.326
TYPE B	X	15	−X	modal	+90.25	0.248
TYPE B	Y	20	+Y	modal	−64.25	0.351

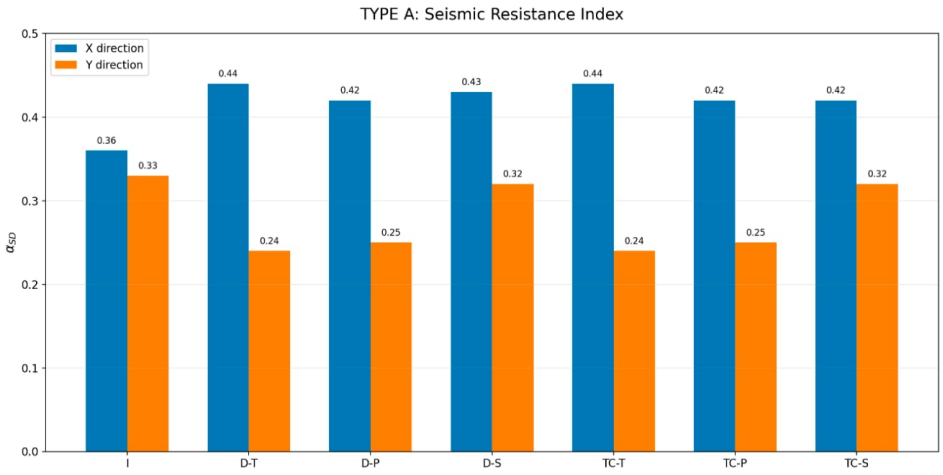


Figure 8. Seismic resistance index αSD for TYPE A in the X and Y directions.

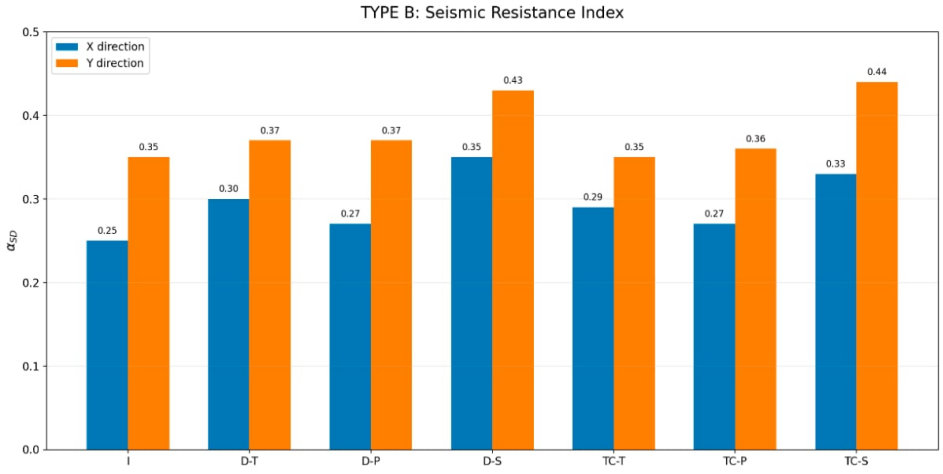


Figure 9. Seismic resistance index αSD for TYPE B in the X and Y directions.

Table 10. Relative change in αSD with respect to the original condition.

Type	Configuration	ΔαSD,X	ΔαSD,Y	Δmin. αSD	Directional Ratio
TYPE A	Original condition (reference)	—	—	—	1.09
TYPE A	Timber panel—attic	+22.2%	−27.3%	−27.3%	1.83
TYPE A	Timber panel—partial	+16.7%	−24.2%	−24.2%	1.68
TYPE A	Timber panel—all above basement	+19.4%	−3.0%	−3.0%	1.34
TYPE A	Timber–concrete composite slab—attic	+22.2%	−27.3%	−27.3%	1.83
TYPE A	Timber–concrete composite slab—partial	+16.7%	−24.2%	−24.2%	1.68
TYPE A	Timber–concrete composite slab—all above basement	+16.7%	−3.0%	−3.0%	1.31
TYPE B	Original condition (reference)	—	—	—	1.40
TYPE B	Timber panel—attic	+20.0%	+5.7%	+20.0%	1.23
TYPE B	Timber panel—partial	+8.0%	+5.7%	+8.0%	1.37
TYPE B	Timber panel—all above basement	+40.0%	+22.9%	+40.0%	1.23

Table 10. *Cont.*

Type	Configuration	ΔαSD,X	ΔαSD,Y	Δmin. αSD	Directional Ratio
TYPE B	Timber–concrete composite slab—attic	+16.0%	0.0%	+16.0%	1.21
TYPE B	Timber–concrete composite slab—partial	+8.0%	+2.9%	+8.0%	1.33
TYPE B	Timber–concrete composite slab—all above basement	+32.0%	+25.7%	+32.0%	1.33

4.3. Polar Distribution of Seismic Capacity

The polar plots confirm that increasing diaphragm stiffness does not produce a uniform radial expansion of capacity. For TYPE A, attic-only and partial interventions alter the shape of the diagram more strongly than comprehensive strengthening, indicating force redistribution and torsional sensitivity. For TYPE B, the comprehensive variants increase the available capacity in both principal directions, whereas the partial variants do not provide proportional improvement. Quantitatively, this is expressed by the ratio αSD,max/αSD,min between the principal directions (Table 10): for TYPE A, the ratio increases from 1.09 in the original condition to 1.83 with attic-only strengthening and returns to 1.31–1.34 with comprehensive strengthening, whereas for TYPE B it decreases from 1.40 to 1.21–1.37. The polar distributions are shown in Figure 10 for TYPE A and Figure 11 for TYPE B.

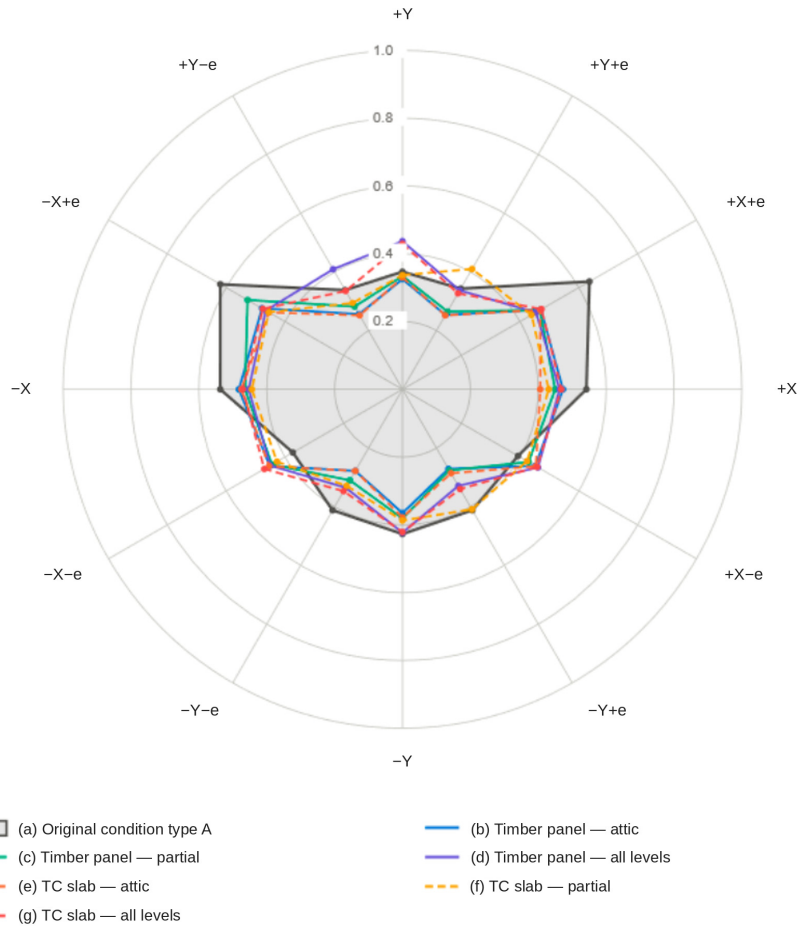


Figure 10. Polar distribution of the seismic resistance index for TYPE A: original condition and six strengthening variants.

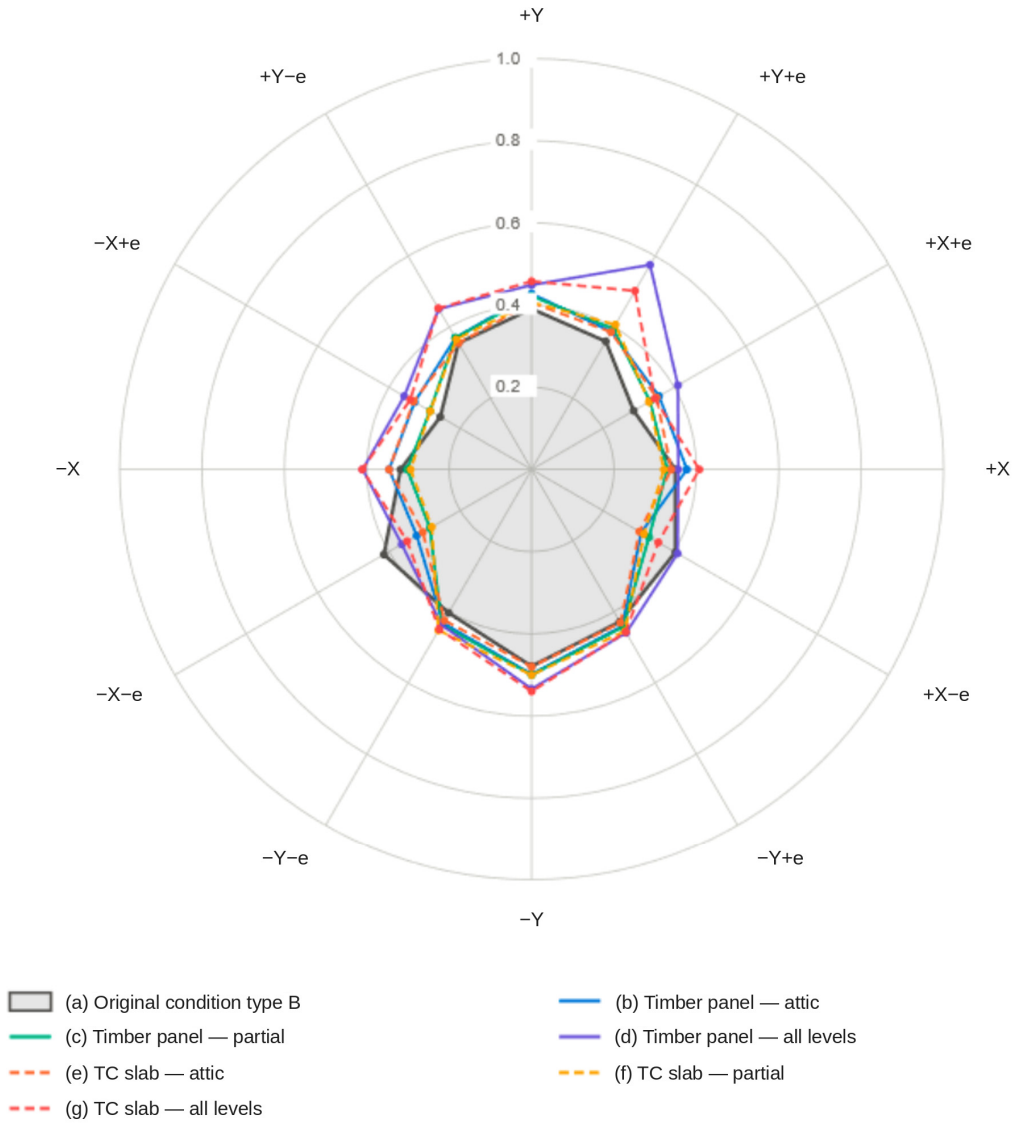


Figure 11. Polar distribution of the seismic resistance index for TYPE B: original condition and six strengthening variants.

4.4. Damage Localisation and Capacity Curves

In the original TYPE A model, the critical mechanism is associated with the staircase wall. After strengthening, damage shifts in all strengthening variants toward the edge wall adjacent to the neighbouring building. This confirms that strengthening the floor can change the governing wall mechanism without increasing the local capacity of the individual wall. The change in critical mechanism is shown in Figure 12.

For TYPE B, the critical element remains the short longitudinal wall in the courtyard zone. Repeated concentration of damage in the same element explains why increasing diaphragm stiffness alone cannot indefinitely increase the global capacity. The critical short longitudinal wall and the associated damage distribution are shown in Figure 13.

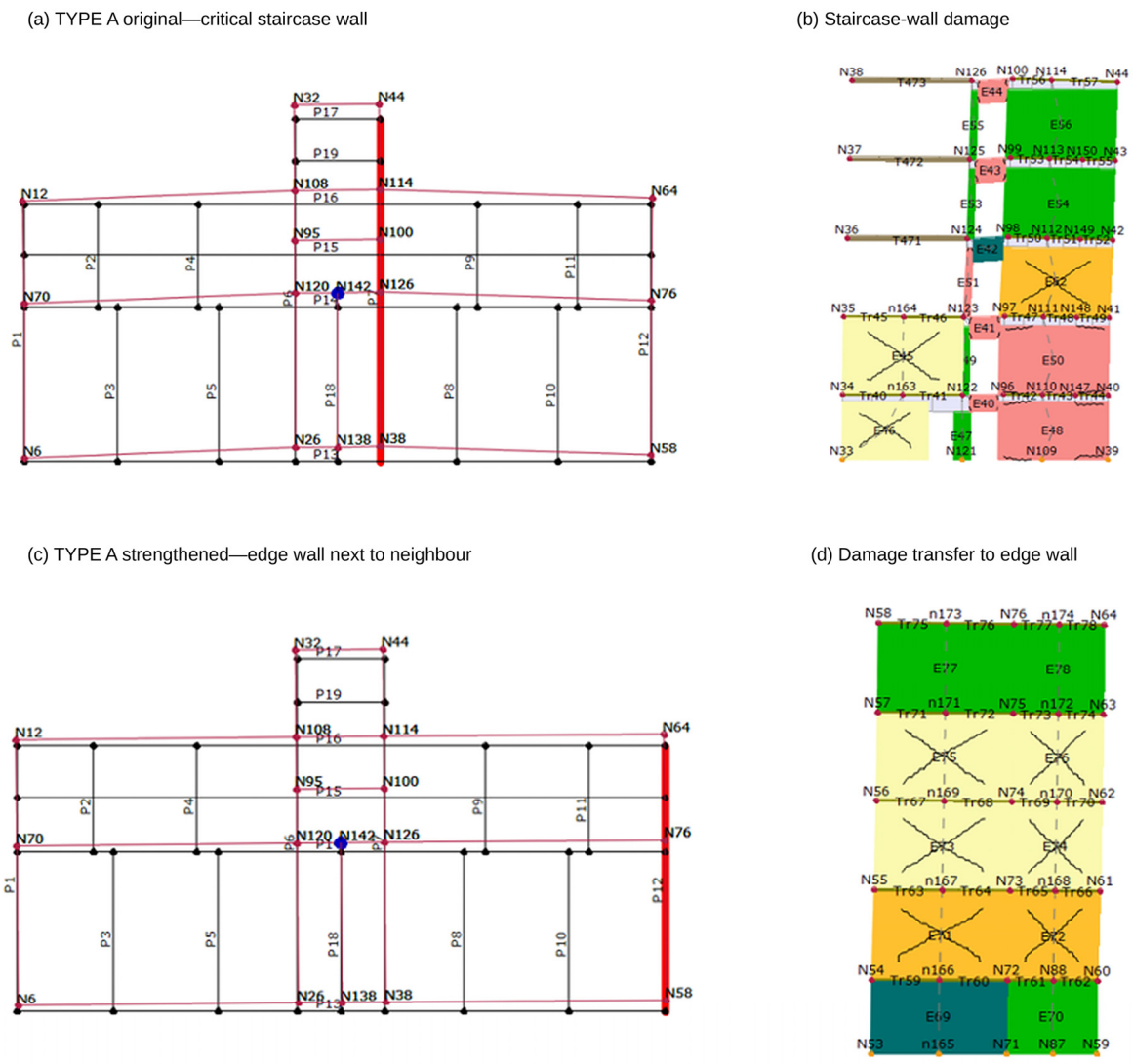


Figure 12. Change in the critical mechanism of TYPE A: original staircase-wall mechanism and shift in damage to the edge wall after strengthening. (**a**) TYPE A original—critical staircase wall; (**b**) staircase-wall damage; (**c**) TYPE A strengthened—edge wall next to the neighbouring building; (**d**) damage transfer to the edge wall. Colours of the masonry elements follow the 3Muri damage legend: green—undamaged; light yellow—shear damage; orange—incipient shear failure; light red—bending damage; dark teal—ineffective element.

The capacity curves confirm that strengthening changes the initial stiffness, modal participation, and the force level at which individual groups of walls are activated. Nevertheless, post-peak degradation and scatter among the pushover analyses remain present. For TYPE B, comprehensive strengthening provides the most favourable capacity-to-demand relationship. For TYPE A, the curves become more uniform, but the unfavourable direction continues to be governed by the existing masonry. The capacity curves are shown in Figure 14 for TYPE A and Figure 15 for TYPE B.

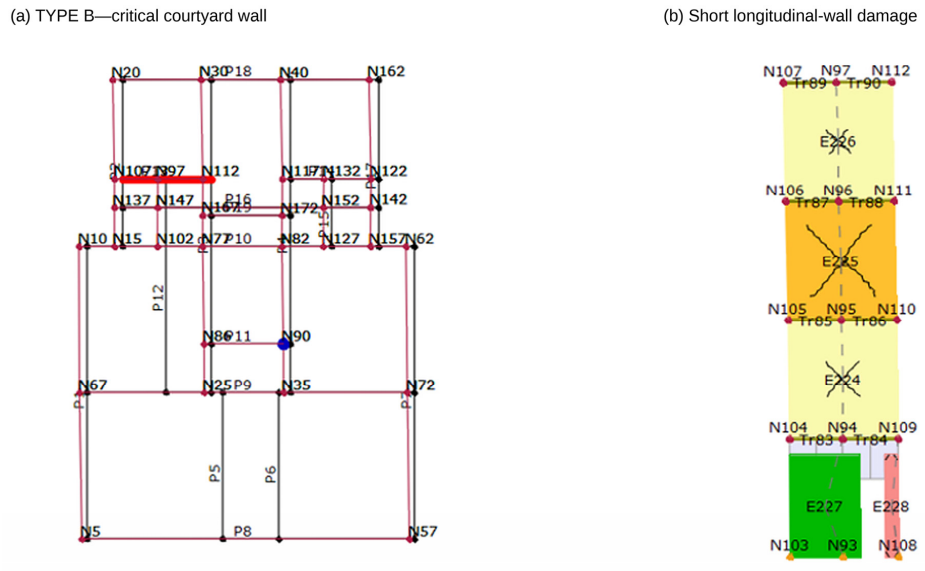


Figure 13. Critical short longitudinal wall in the courtyard zone of TYPE B and the associated damage distribution. (**a**) TYPE B—critical courtyard wall; (**b**) damage of the short longitudinal wall. Colours of the masonry elements follow the 3Muri damage legend, as in Figure 12.

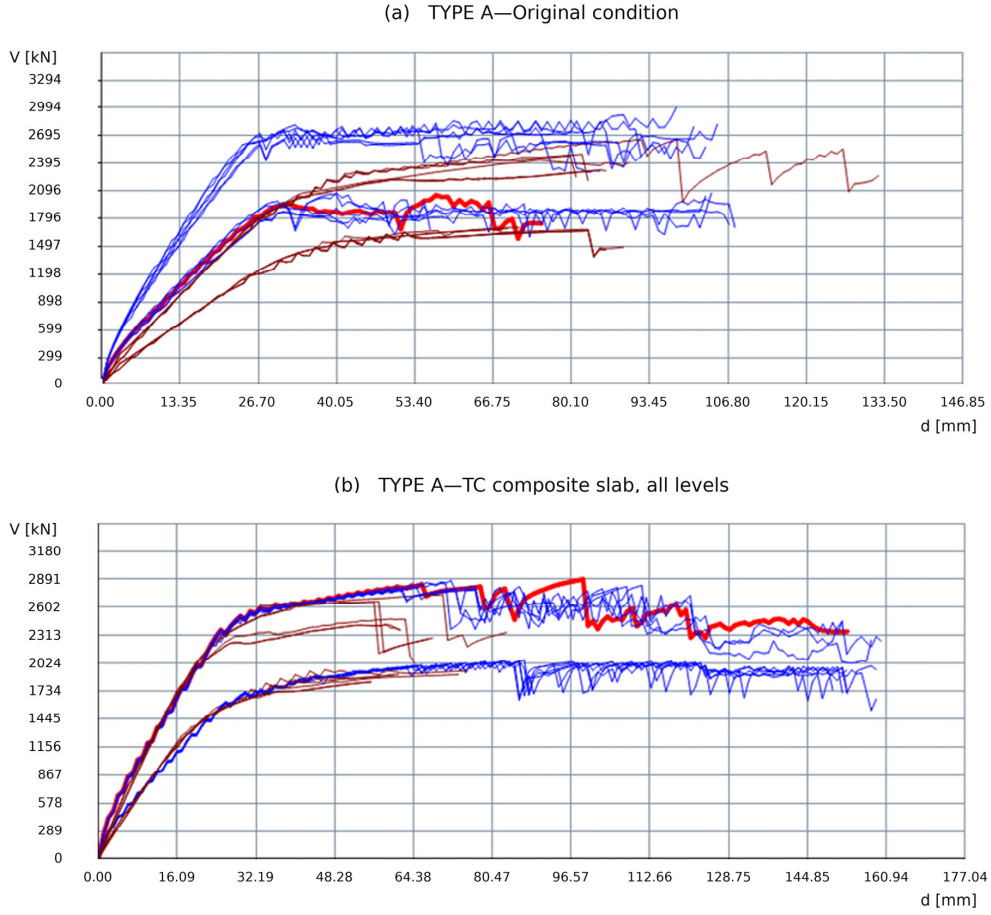


Figure 14. Capacity curves for TYPE A: (**a**) original condition; (**b**) strengthening of all levels above the basement with a timber–concrete composite slab. Blue curves represent pushover analyses in the X direction, dark red curves represent analyses in the Y direction, and the bold red curve highlights the governing pushover analysis.

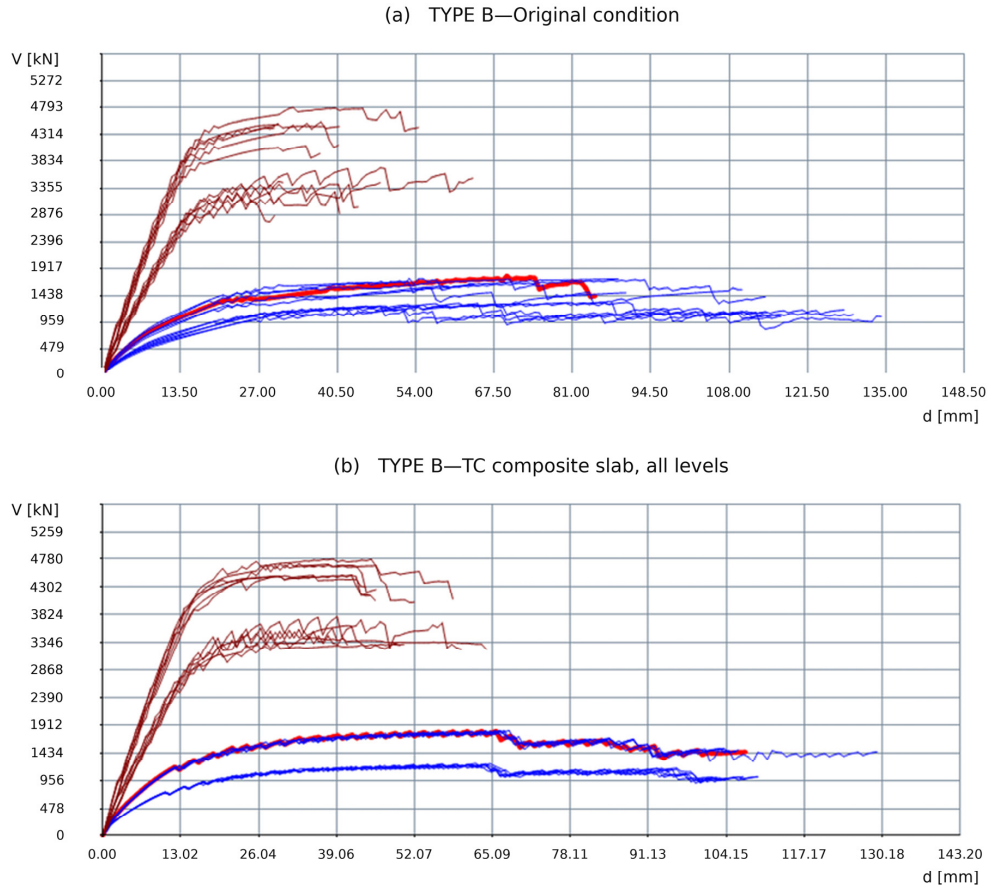


Figure 15. Capacity curves for TYPE B: (**a**) original condition; (**b**) strengthening of all levels above the basement with a timber–concrete composite slab. Blue curves represent pushover analyses in the X direction, dark red curves represent analyses in the Y direction, and the bold red curve highlights the governing pushover analysis.

The governing walls, truncation steps, and failure modes of all configurations are summarised in Table A1 (Appendix A). For TYPE A, the X direction is governed in all seven configurations by the same longitudinal façade wall (wall 13), with predominantly flexural (rocking) damage of the piers, failure of spandrels, and shear failure of a single pier; floor strengthening does not change this mechanism but increases the displacement at which it is reached ($d_{m,X}$ from 45.0 mm to 53–71 mm). In the Y direction, the original model is governed by mixed shear–flexural damage of the staircase wall (wall 7), whereas in all six strengthened variants the critical mechanism becomes shear failure of the piers in the lowest levels of an end wall adjacent to the neighbouring building (wall 12, or the opposite end wall 1 for TC-T), which is reached at a smaller displacement ($d_{m,Y}$ = 38–50 mm instead of 61.3 mm). The stiffer diaphragm therefore redistributes the storey shear towards the end walls, and the reduction in the governing α_{SD} of TYPE A is associated with an earlier, brittle shear mechanism in these walls rather than with a loss of global strength. For TYPE B, the X direction is governed by shear in the short courtyard wall (wall 13; the adjacent courtyard wall 14 for D-S). Attic-only strengthening moves the shear failure of this wall from the first floor to the top storey, directly below the strengthened attic diaphragm, whereas comprehensive strengthening distributes damage over the upper storeys and delays it ($d_{m,X} \approx 51$ mm instead of 40.7 mm). The Y direction of TYPE B is governed in all configurations by shear in wall 12 at practically the same displacement ($d_{m,Y}$ = 22.4–27.2 mm).

4.5. Behaviour Under Vertical Actions

The serviceability limit state is the dominant constraint for the original structure. Of the 144 combinations, 85 satisfy the ULS, but only 69 satisfy the SLS; every combination satisfying the SLS also satisfies the ULS. The number of combinations satisfying both criteria decreases from 24 at a span of 3.5 m to one at a span of 6.0 m. The number of combinations satisfying the individual limit states is given in Table 11. A supplementary check of the original joists that includes creep (final deflection with kdef = 0.60 and $\psi 2 = 0.30$ [56], limit L/250) reduces the number of combinations satisfying the SLS from 69 to 55, which confirms that long-term deformation further restricts the admissible spans of the existing floors.

Table 11. Number of cross-section and span combinations satisfying the limit states (out of 144).

System	ULS Count	ULS (%)	SLS Count	SLS (%)	ULS and SLS Count	ULS and SLS (%)
Original joist	85	59.0	69	47.9	69	47.9
Timber panel 2 × 30 mm	99	68.8	106	73.6	99	68.8
Timber–concrete composite slab 80 mm	122	84.7	144	100.0	122	84.7

The cross-laid timber panel, in which only the layer parallel to the joists acts compositely, increases the number of combinations satisfying both criteria from 69 to 99. Unlike in the original condition, the ULS becomes governing: 99 combinations satisfy the ULS and 106 the SLS, and every combination satisfying the ULS also satisfies the SLS. The governing check is combined bending and tension of the existing joist at $t = \infty$. For the representative 200 × 240 mm joist at a 5.0 m span, utilisation decreases from 90% for ULS and 107% for SLS to 80% and 70%, respectively; at a 6.0 m span, both limit states are exceeded (111% and 112%). When creep is included (final deflection, limit L/250), 84 combinations satisfy both the ULS and the final-deflection criterion. Utilisation ratios of the representative joist for the analysed spans are given in Table 12.

Table 12. Utilisation of the representative 200 × 240 mm joist.

System	ULS 5.0 m	SLS 5.0 m	ULS 5.5 m	SLS 5.5 m	ULS 6.0 m	SLS 6.0 m
Original condition	90%	107%	109%	142%	129%	184%
Timber panel 2 × 30 mm	80%	70%	95%	90%	111%	112%
Timber–concrete composite slab 80 mm	65%	38%	78%	47%	91%	58%

The TCC slab with an 80 mm concrete layer provides the most effective deflection control. All 144 combinations satisfy the SLS, while 122 satisfy the ULS. This result refers to idealised, initially straight joists with the assumed connector properties and does not account for existing sag, deterioration of the existing timber, or the fresh-concrete stage; it should therefore not be read as a guarantee of serviceability for an actual floor (see Sections 5.4 and 5.6). The governing criterion generally shifts to the shear resistance of the screws. For the 200 × 240 mm joist, SLS utilisation at spans of 5.0, 5.5, and 6.0 m decreases to 38%, 47%, and 58%, respectively.

5. Discussion

5.1. Influence of Continuity and Nominal Stiffness

For the analysed models, the principal result is that the extent and continuity of the intervention have a stronger influence on the global response than the difference between the two strengthening systems considered. The timber and timber–concrete composite variants produce similar αSD values when applied over the same area, even though the nominal stiffness of the composite slab is substantially greater. Once sufficiently effective diaphragm action is established, the unstrengthened walls become the governing elements of the system. It should also be emphasised that all obtained αSD values lie between 0.24 and 0.44; therefore, no model—neither the original nor the comprehensively strengthened one—reaches the seismic demand for a return period of 475 years. All values are also below αSD = 0.50, the minimum threshold for Level 2 rehabilitation according to the Technical Regulation [34]. Floor strengthening therefore changes force distribution, load paths, and the global response, but without wall strengthening it does not bring the analysed building types to the required level.

In the analysed configuration, partial asymmetric strengthening did not represent a linear intermediate stage between the original and comprehensively strengthened conditions. The strengthened portion transfers horizontal action more effectively, while the adjacent flexible portion retains larger in-plane deformations. The results indicate a change in stiffness distribution and increased rotational sensitivity of the storey, accompanied by a change in the load path toward the walls. This interpretation is consistent with the unfavourable results of the analysed partial variants for TYPE A and the reduction in αSD,X for the TYPE B partial variants compared with attic-only strengthening. Because only one location and extent of plan-asymmetric strengthening (one half of the floor above the first storey) was examined, these observations should not be generalised to asymmetric interventions as such; other locations, extents, and combinations of strengthened zones may lead to different trends.

Despite the approximately 108-fold (timber panel) and 2583-fold (composite slab) increases in membrane shear stiffness Gt relative to the original floor (Section 3.4), the differences in αSD between timber and composite variants applied over the same intervention extent remain small: the governing αSD differ by at most 0.02 (Table 8). Because G_t of the composite slab is approximately 18 times that of the timber panel, this comparison also brackets the sensitivity of the results to the membrane stiffness of the strengthened diaphragm: a change of more than one order of magnitude in G_t has practically no influence on the governing αSD once diaphragm action is established. Table A1 shows that, for the same intervention extent, both systems are governed by the same type of mechanism in the same zone of the building.

5.2. Relationship Between Diaphragm Stiffness and Masonry Capacity

A larger participating mass indicates more coherent global participation but does not imply greater wall strength. A very stiff diaphragm can more clearly activate previously less-loaded weak walls because it transfers forces more efficiently. The shift in the critical mechanism in TYPE A and the persistently critical short wall in TYPE B support this interpretation.

The αSD index should therefore be interpreted together with the shape of the capacity curve and the localisation of damage. An increase in base shear or αSD may occur simultaneously with a locally unacceptable brittle mechanism. A comprehensive rehabilitation assessment must include verification of in-plane wall behaviour, wall–floor connections, local out-of-plane mechanisms, and the vertical load-bearing capacity of walls and foun-

dations, while respecting the principles of minimum intervention and compatibility with cultural heritage [59].

5.3. Timber Panel Versus TCC Slab

The timber panel provides a substantial increase in diaphragm action with a lower panel self-weight than the concrete compression layer; however, the actual net mass change depends on the removed and newly added floor layers. It is suitable for dry construction, offers greater reversibility, and is more compatible with historic materials. Its vertical effect is significant, but because only the layer parallel to the joists acts compositely, at larger spans it is limited by the bending and tension resistance of the existing joists, fastener slip, and long-term deformation.

The timber–concrete composite slab controls deflection considerably more effectively and brings the behaviour closer to that of a rigid diaphragm. The final balance of permanent load depends on the amount of fill removed and the new floor build-up and must be determined for each specific building. During concreting, the existing joists and temporary props carry the fresh concrete before composite action is established.

A life-cycle assessment was not performed in this study. Consequently, no environmental superiority of either system is claimed; instead, the structural trade-offs relevant to sustainable rehabilitation are considered: quantity of new material, additional mass, reversibility, moisture risk, preservation of historic fabric, and the possibility of retaining the existing joists. A qualitative comparison of the two systems is given in Table 13.

Table 13. Qualitative comparison of the strengthening systems considered.

Criterion	Timber Panel 2 × 30 mm	Timber–Concrete Composite Slab 80 mm
Seismic effect in the analysed models	Comparable to the composite slab for the same intervention extent	Comparable to the timber panel for the same intervention extent
Stiffness under vertical actions	Moderate increase	Large increase
Long-term deflection	May remain governing at large spans	Generally not governing within the analysed range
Governing local limitation	Bending and tension of the existing joists; long-term deformation	Shear in fasteners for slender joists
Additional mass	Low	Higher and dependent on the specific floor build-up
Construction method	Dry and potentially reversible process	Wet, staged, and difficult-to-reverse process
Compatibility with heritage fabric	Generally more favourable	Requires more detailed justification
Main design risk	Insufficient SLS improvement	Force concentration in masonry and loads during construction

5.4. Existing Deflections and Construction Stages

The analysis under vertical actions is based on idealised initially straight joists. In actual structures more than 100 years old, part of the deflection has already developed because of creep, moisture variations, support deformation, local damage, and settlement. Without geometric measurements, satisfying the SLS for the strengthened section does not demonstrate that the finished floor will be level or that the total existing deflection will be acceptable.

If strengthening is installed in the existing deformed configuration, it primarily reduces future increments of deflection while the existing sag remains. If unloading and lifting of the

structure are planned, the recoverable part of the deformation and the forces introduced during lifting must be assessed. Excessive levelling may damage timber, wall bearings, ceilings, and partition walls. Three-dimensional surveying is recommended before intervention.

For the TCC slab, the fresh-concrete stage must be checked separately. A simplified check of the unpropped stage, in which the existing joists alone carry the residual floor layers (assumed 0.5 kN/m^2), the fresh concrete (2.0 kN/m^2), and a construction load of 0.75–1.5 kN/m^2 according to EN 1991-1-6 [60], indicates that 7–22 of the 144 combinations—all with spans of 5.0 m or more—would exceed the bending resistance of the joists, and that 22 combinations would develop locked-in deflections exceeding L/300 before composite action is established. Temporary propping is therefore a prerequisite for these combinations, and the locked-in deflection of the joists should be considered in the final SLS verification. For the timber panel, the assumed degree of composite action (γ-method with the adopted slip moduli) depends on the quality of contact, screw installation, and the condition of the existing timber. For both systems, connection testing or conservative slip parameters are recommended.

5.5. Interpretation Framework and Transferability of Results

The methodological strategy of this study is comparative. Geometry, masonry properties, seismic demand, and nonlinear-analysis settings were kept identical within each building type, while only the type and spatial extent of floor strengthening were systematically varied. This reduces the influence of uncontrolled differences between models and allows direct comparison of relative changes in modal response, αSD, and damage localisation.

Because neither experimental validation nor an additional sensitivity analysis was performed, the most reliable conclusions concern the direction and relative magnitude of change within the same building type. Absolute capacity values should not be transferred to a specific building without investigative works. Several features of the results nevertheless limit the influence of the main modelling uncertainties on the relative conclusions. First, the masonry properties correspond to central values of code-recommended ranges and of Croatian flat-jack data (Section 3.3) and were identical in all configurations of a type. Second, the timber and composite variants differ by a factor of approximately 18 in membrane shear stiffness, yet their governing αSD differ by at most 0.02 (Section 5.1), so that moderate uncertainty in the diaphragm stiffness is not expected to change the ranking of the configurations. Third, the total seismic mass changed by less than 5% in all variants (Section 3.4); in particular, the attic-only composite variants retain the original mass within 0.1% and thus effectively represent a scenario with strengthened stiffness and original mass, yet they produce the same changes in αSD as the attic-only timber variants (e.g., +22.2% in αSD,X and −27.3% in αSD,Y for TYPE A). The reported changes in αSD are therefore attributable mainly to the changed stiffness distribution rather than to the change in mass.

5.6. Limitations of the Study

The study was designed to isolate and quantify the influence of different levels of floor stiffness on the seismic response of existing unreinforced masonry buildings. Accordingly, some aspects of actual structural behaviour were intentionally simplified or were not included in the model. The principal limitations can be summarised as follows:

- Two typological models were analysed. They do not encompass the full geometric, structural, and material diversity of the existing Zagreb building stock, but they represent typical buildings affected by the Zagreb earthquake.
- The mechanical properties of masonry and timber were not determined by tests on the specific modelled buildings; conservative reference values were adopted instead. No quantitative sensitivity analysis with respect to the masonry stiffness and strength

was performed; the absolute αSD values, and possibly the location of the critical walls, are conditional on the adopted central values (Section 3.3), whereas the relative comparison between configurations is expected to be less affected because the same values were used in all configurations.

- The equivalent-frame model does not explicitly represent all local failure mechanisms, including out-of-plane wall failure, local anchor failure, connection degradation, and detailed nonlinear behaviour of the floor diaphragms.
- Existing long-term deflections, vibrations, actual stiffness, and the degree of degradation of timber joists and their connections were not determined experimentally. This is particularly important for floors several decades old, for which seismic improvement of diaphragm action does not necessarily imply adequate strength and serviceability under vertical actions.
- The walls in the analysed models were not additionally strengthened. The results therefore represent the isolated contribution of interventions on the floors rather than the behaviour of the building after comprehensive structural or seismic rehabilitation.
- The N2 method reduces a multi-degree-of-freedom system to an equivalent single-degree-of-freedom system and is most reliable when the response is governed by a stable fundamental mode. For strongly plan- or vertically irregular buildings, or systems with a significant contribution from higher modes, the results may require additional verification using more advanced nonlinear static or dynamic procedures. This limitation is particularly relevant to TYPE A in the original condition, in which the first Y-dominant mode activates 43.79% of the mass and the X-dominant response appears only in the sixth mode, and to the plan-asymmetric variants, in which strengthening intentionally modifies the torsional and three-dimensional response. Multimodal or adaptive pushover procedures and nonlinear time-history analyses with sets of representative ground-motion records were beyond the scope of this comparative study and are planned for future work. The absolute αSD values should therefore be interpreted with caution, whereas the relative comparison between variants is expected to be less affected because the same procedure and settings were applied to all models. In Croatian post-earthquake assessment practice, the N2 method is the standard procedure.
- Strengthening modifies both the diaphragm stiffness and the seismic mass, because the rubble fill is removed in some variants and a concrete layer is added in others (Section 3.2). The total seismic mass changed by only −0.1% to −4.1% (Section 3.4), so the stiffness effect dominates the comparisons; however, the vertical redistribution of mass (e.g., removal of the rubble fill at the attic level in the timber variants) was not separated from the stiffness change in dedicated analyses.
- The models assume a fixed base at the foundation level. Soil–structure interaction, foundation flexibility, and differential settlement were not considered, although ground type C was adopted for the seismic demand. For historic masonry buildings with basements, foundation compliance may modify the modal response, torsional behaviour, and wall demand; these effects should be addressed in future extensions of the framework.

In the strengthened-floor models, the assumptions of "adequately connected joists" and a "surface fixed into the masonry" idealise effective force transfer between the diaphragm and the walls. Anchor slip or yielding, local masonry failure at bearing zones, wall–floor separation, and degradation of existing connections were not modelled explicitly. The results therefore estimate the potential diaphragm effect under the assumption of a properly executed connection with adequate capacity, rather than verifying a specific anchorage detail. This assumption affects the principal conclusions: if anchor slip, wall–floor separa-

tion, or local masonry failure at the bearing zones occurred before the global mechanism developed, force transfer between the diaphragm and the walls would be less effective than modelled, and the changes in αSD reported for the strengthened variants—whether favourable or unfavourable—may be overestimated. In addition, the equivalent-frame model does not capture out-of-plane mechanisms of façade and gable walls, which were among the predominant damage modes in the 2020 earthquakes [5,10,11]. Strengthened and properly anchored diaphragms are expected to restrain these mechanisms, but their verification requires separate local (kinematic) analyses of the wall–floor system, which are beyond the scope of this study. The reported results should therefore be read as conditional on the provision of wall–floor connections with adequate stiffness and capacity. Additional epistemic uncertainty is introduced by the manual truncation of selected capacity curves when an important wall enters the Significant Damage state. This procedure requires engineering judgement regarding the possibility of further force redistribution and preservation of the vertical load path. Although the same criterion was applied consistently to all analysed models, future studies should quantify the sensitivity of αSD and of the ranking of the configurations to alternative truncation criteria. Because the truncation point precedes a 20% drop of the base shear in all governing analyses, alternative criteria would generally yield larger dm and αSD values, particularly in the X direction, where truncation occurred at about one third to one half of the analysis steps for TYPE B (Table A1). The truncation step, the governing wall, and the corresponding displacement capacity are reported for all governing analyses in Table A1 to make this judgement traceable.

6. Conclusions

The results show that attic-only strengthening or partial strengthening of floor structures cannot automatically be associated with a proportional increase in the overall seismic resistance of the building. The effect of the intervention depends strongly on the existing stiffness distribution, the position of the strengthened level, and the continuity of force transfer through the structure. This was particularly evident for TYPE A, where attic-level strengthening improved the response in the X direction while simultaneously reducing αSD in the Y direction by 27.3%. Similarly, for the single analysed location and extent of plan-asymmetric strengthening of one half of the floor above the first storey, no greater improvement was achieved than with attic-only strengthening. In this case, stiffness discontinuity and the altered force-transfer path had a greater influence on the global response than the mere increase in strengthened floor area. The results therefore indicate that, at least for the analysed configurations, partial strengthening can also have adverse consequences if it is not considered in the context of the overall three-dimensional behaviour of the building.

The most balanced global response was achieved by comprehensive strengthening of all levels above the basement. For TYPE B, the minimum directional αSD increased by 40% with the timber panel and by 32% with the timber–concrete composite slab. However, the TYPE A results show that a more balanced response does not necessarily imply an increase in the governing structural capacity. Even after comprehensive strengthening, the minimum directional αSD was 0.32 compared with 0.33 in the original condition. This indicates that improved diaphragm action can redistribute forces more favourably and reduce the severity of certain irregularities, but it cannot compensate for insufficient capacity of the vertical structural elements that become governing after floor strengthening.

In the analysed models, the timber and TCC floors produced relatively similar global seismic indicators when the same intervention extent was used. Differences in minimum αSD between the two systems for the same strengthening extent remained within approximately 6%. This shows that, once sufficiently effective diaphragm action is established, further increases in floor stiffness do not necessarily translate into a comparable increase

in global seismic resistance because the unstrengthened walls and their capacity become governing. From the perspective of seismic response, the choice of floor strengthening system should therefore not be based solely on achieving the maximum possible stiffness.

Differences between the systems considered are more pronounced under vertical actions. Both analysed limit states were satisfied by 47.9% of combinations in the original condition, 68.8% with the timber panel, and 84.7% with the timber–concrete composite slab. The timber panel provides a lightweight and potentially reversible solution, which is especially important for historic buildings; however, the resistance of the existing joists and long-term deflection remain governing at larger spans. The TCC slab more effectively increases flexural stiffness and controls deflection, but it also introduces additional mass and requires reliable composite action, verification of connections and construction stages, and confirmation that the existing masonry can accommodate increased local and global actions. The vertical-analysis results should therefore be interpreted as a relative comparison of the effectiveness of the systems considered under identical input assumptions rather than as a final assessment of an actual historic floor, because existing long-term deflections and the actual condition of the joists were not measured, as identified in the study limitations.

Overall, the results confirm that floor strengthening should be treated as part of an integrated structural rehabilitation concept rather than as an isolated measure. The design solution must simultaneously consider wall capacity, the quality and capacity of wall–floor connections, local out-of-plane mechanisms, continuity of the vertical load path, changes in plan and vertical regularity, and construction stages. The conclusions of this study therefore provide a relative comparison of the analysed numerical configurations and identify trends in structural behaviour, but they cannot replace building-specific investigations and design checks. All seismic findings are conditional on the assumption of effective wall–floor connections and were obtained with the N2 method, whose limitations for responses with significant higher-mode and torsional contributions are discussed in Section 5.6. All calculated directional seismic resistance indices lie between 0.24 and 0.44, so none of the analysed variants reaches $\alpha SD = 1.00$ for the 475-year seismic demand. Moreover, none reaches the minimum $\alpha SD = 0.50$ threshold prescribed for Level 2 rehabilitation under the Croatian Technical Regulation [34]. This indicates that improving floor diaphragm action alone, without simultaneous intervention on insufficiently resistant walls and their connections, is not sufficient to achieve the target seismic resistance.

Supplementary Materials: The following supporting information can be downloaded at: https://www.mdpi.com/article/10.3390/buildings16234747/s1. Table S1—complete utilisation matrix for ULS and SLS of the original timber joists; Table S2—complete utilisation matrix for joists strengthened with a cross-laid 2 × 30 mm GL24h timber panel (30 mm composite flange); Table S3—complete utilisation matrix for joists strengthened with a timber–concrete composite slab with an 80 mm C25/30 concrete layer.

Author Contributions: Conceptualization, I.V.; methodology, I.V.; software, I.V. and D.Č.; formal analysis, I.V. and M.S.; investigation, I.V. and Š.S.; data curation, D.Č.; writing—original draft preparation, I.V.; writing—review and editing, I.V. and M.S.; visualization, Š.S. and M.S.; supervision, M.S. All authors have read and agreed to the published version of the manuscript.

Funding: This research received no external funding.

Institutional Review Board Statement: Not applicable.

Informed Consent Statement: Not applicable.

Data Availability Statement: The data supporting the findings of this study are contained within the article and the Supplementary Materials. Additional numerical model files are available from the corresponding author upon reasonable request.

Conflicts of Interest: Dean Čizmar serves as a Guest Editor of the Special Issue to which this manuscript is submitted. In accordance with MDPI editorial policy, he will not participate in the editorial handling, peer-review process, or decision-making for this manuscript. The other authors declare no conflicts of interest.

Appendix A

Table A1 lists, for each configuration and direction, the governing pushover analysis according to the minimum αSD, the wall in which the truncation criterion of Section 3.5 was reached, the analysis step at truncation relative to the total number of steps, the resulting displacement capacity dm, and the damage state of the governing wall at that step according to the damage classification of 3Muri (incipient shear failure, shear failure, ineffective element). Wall numbers refer to the 3Muri models.

Table A1. Governing analyses, truncation steps, displacement capacities, and failure mechanisms of all configurations.

Type	Config.	Dir.	Analysis	Wall	Step at Truncation/Total	dm (mm)	Governing Wall and Failure Mode at Truncation
A	I	X	16	13	46/57	45.00	Façade wall: flexure of piers, spandrel failure, shear failure of one pier
A	I	Y	19	7	63/71	61.30	Staircase wall: mixed shear and flexure of lower-storey piers
A	D-T	X	16	13	71/113	69.97	As I-X
A	D-T	Y	19	12	40/43	38.31	End wall: shear; basement piers ineffective, ground-floor piers at incipient shear failure
A	D-P	X	12	13	66/114	65.02	As I-X
A	D-P	Y	19	12	41/43	39.76	As D-T-Y
A	D-S	X	14	13	54/169	53.98	As I-X
A	D-S	Y	23	12	50/62	50.31	End wall: shear; ground-floor pier ineffective, first-floor pier at incipient shear failure
A	TC-T	X	12	13	71/109	71.03	As I-X
A	TC-T	Y	20	1	39/43	38.85	Opposite end wall: shear; basement piers ineffective, ground-floor piers at incipient shear failure
A	TC-P	X	12	13	66/131	66.01	As I-X
A	TC-P	Y	19	12	39/43	38.80	As D-T-Y
A	TC-S	X	10	13	53/116	53.02	As I-X
A	TC-S	Y	19	12	48/57	47.75	End wall: shear; basement piers ineffective, first-floor piers at incipient shear failure

Table A1. *Cont.*

Type	Config.	Dir.	Analysis	Wall	Step at Truncation/Total	dm (mm)	Governing Wall and Failure Mode at Truncation
B	I	X	15	13	51/169	40.74	Short courtyard wall: shear, incipient shear failure of first-floor pier
B	I	Y	20	12	28/38	22.45	Shear; ground-floor pier ineffective, incipient shear failure at first floor; spandrels in flexure
B	D-T	X	12	13	55/142	44.07	Short courtyard wall: shear failure of top-storey pier
B	D-T	Y	20	12	29/38	22.44	As I-Y
B	D-P	X	16	13	54/160	43.13	As I-X
B	D-P	Y	20	12	28/41	22.44	As I-Y
B	D-S	X	11	14	64/125	51.28	Adjacent courtyard wall: shear, incipient shear failure of first- and second-floor piers
B	D-S	Y	24	12	33/50	26.36	Shear; incipient shear failure at first floor, ground-floor pier damaged in shear
B	TC-T	X	12	13	54/148	43.28	As D-T-X
B	TC-T	Y	20	12	29/38	22.44	As I-Y
B	TC-P	X	16	13	53/159	42.33	As I-X
B	TC-P	Y	20	12	28/43	22.44	As I-Y
B	TC-S	X	15	13	64/135	51.12	As I-X
B	TC-S	Y	24	12	34/50	27.16	As D-S-Y

Note: Configuration designations as in Table 2. Floor levels are counted from the basement (basement, ground floor, first floor, ...). "As I-X", etc. denotes the same wall and the same type of mechanism as in the indicated row.

References

1. Atalić, J.; Šavor Novak, M.; Uroš, M. Seismic Risk for Croatia: Overview of Research Activities and Present Assessments with Guidelines for the Future. *Građevinar* **2019**, *71*, 923–947. [CrossRef]
2. Šavor Novak, M.; Uroš, M.; Atalić, J.; Herak, M.; Demšić, M.; Baniček, M.; Lazarević, D.; Bijelić, N.; Crnogorac, M.; Todorić, M. Zagreb Earthquake of 22 March 2020—Preliminary Report on Seismologic Aspects and Damage to Buildings. *Građevinar* **2020**, *72*, 843–867. [CrossRef]
3. Volarić, I.; Stepinac, M. The Influence of Floor Structures on the Seismic Response of Unreinforced Masonry Buildings from the Late 19th and Early 20th Century in Zagreb. *Građevinar* **2026**, *78*, 339–353. (In Croatian) [CrossRef]
4. Atalić, J.; Uroš, M.; Šavor Novak, M.; Demšić, M.; Nastev, M. The Mw5.4 Zagreb (Croatia) Earthquake of March 22, 2020: Impacts and Response. *Bull. Earthq. Eng.* **2021**, *19*, 3461–3489. [CrossRef] [PubMed]
5. Stepinac, M.; Lourenço, P.B.; Atalić, J.; Kišiček, T.; Uroš, M.; Baniček, M.; Šavor Novak, M. Damage Classification of Residential Buildings in Historical Downtown after the ML5.5 Earthquake in Zagreb, Croatia in 2020. *Int. J. Disaster Risk Reduct.* **2021**, *56*, 102140. [CrossRef]
6. Markušić, S.; Stanko, D.; Korbar, T.; Belić, N.; Penava, D.; Kordić, B. The Zagreb (Croatia) M5.5 Earthquake on 22 March 2020. *Geosciences* **2020**, *10*, 252. [CrossRef]

7. Perić, L.; Matorić, I. Reliability of Traditional Timber-Floor Masonry Buildings to Seismic Action. *Građevinar* **2020**, *72*, 869–893. [CrossRef]
8. Bruneau, M. State-of-the-Art Report on Seismic Performance of Unreinforced Masonry Buildings. *J. Struct. Eng.* **1994**, *120*, 230–251. [CrossRef]
9. Penna, A.; Morandi, P.; Rota, M.; Manzini, C.F.; da Porto, F.; Magenes, G. Performance of Masonry Buildings during the Emilia 2012 Earthquake. *Bull. Earthq. Eng.* **2014**, *12*, 2255–2273. [CrossRef]
10. Sorrentino, L.; D'Ayala, D.; de Felice, G.; Griffith, M.C.; Lagomarsino, S.; Magenes, G. Review of Out-of-Plane Seismic Assessment Techniques Applied to Existing Masonry Buildings. *Int. J. Archit. Herit.* **2017**, *11*, 2–21. [CrossRef]
11. Jajčević, K.; Demšić, M.; Šavor Novak, M.; Atalić, J.; Uroš, M. Overturning of Unreinforced Masonry Walls—Predominant Failure Mechanism in Historic Masonry Buildings. *Građevinar* **2025**, *77*, 1057–1069. [CrossRef]
12. Ožić, K. Refining Seismic Vulnerability Models for Historic Masonry Buildings through Parametric Numerical Analysis. *Resil. Reuse Built Environ.* **2026**, e0005. [CrossRef]
13. Wilson, A.; Quenneville, P.J.H.; Ingham, J.M. In-Plane Orthotropic Behavior of Timber Floor Diaphragms in Unreinforced Masonry Buildings. *J. Struct. Eng.* **2014**, *140*, 04013038. [CrossRef]
14. Brignola, A.; Pampanin, S.; Podestà, S. Experimental Evaluation of the In-Plane Stiffness of Timber Diaphragms. *Earthq. Spectra* **2012**, *28*, 1687–1709. [CrossRef]
15. Tomić, I.; Vanin, F.; Božulić, I.; Beyer, K. Numerical Simulation of Unreinforced Masonry Buildings with Timber Diaphragms. *Buildings* **2021**, *11*, 205. [CrossRef]
16. Ruggieri, S.; Porco, F.; Uva, G. A Numerical Procedure for Modeling the Floor Deformability in Seismic Analysis of Existing RC Buildings. *J. Build. Eng.* **2018**, *19*, 273–284. [CrossRef]
17. Ruggieri, S.; Porco, F.; Uva, G. A Practical Approach for Estimating the Floor Deformability in Existing RC Buildings: Evaluation of the Effects in the Structural Response and Seismic Fragility. *Bull. Earthq. Eng.* **2020**, *18*, 2083–2113. [CrossRef]
18. Piazza, M.; Baldessari, C.; Tomasi, R. The Role of In-Plane Floor Stiffness in the Seismic Behaviour of Traditional Buildings. In Proceedings of the 14th World Conference on Earthquake Engineering, Beijing, China, 12–17 October 2008.
19. Valluzzi, M.R.; Garbin, E.; Dalla Benetta, M.; Modena, C. In-Plane Strengthening of Timber Floors for the Seismic Improvement of Masonry Buildings. In Proceedings of the World Conference on Timber Engineering, Riva del Garda, Italy, 20–24 June 2010.
20. Mirra, M.; Ravenshorst, G. Optimizing Seismic Capacity of Existing Masonry Buildings by Retrofitting Timber Floors: Wood-Based Solutions as a Dissipative Alternative to Rigid Concrete Diaphragms. *Buildings* **2021**, *11*, 604. [CrossRef]
21. Mirra, M.; Ravenshorst, G.; van de Kuilen, J.-W. Comparing In-Plane Equivalent Shear Stiffness of Timber Diaphragms Retrofitted with Light and Reversible Wood-Based Techniques. *Pract. Period. Struct. Des. Constr.* **2021**, *26*, 04021031. [CrossRef]
22. Moreira, S.; Ramos, L.F.; Oliveira, D.V.; Lourenço, P.B. Experimental Behavior of Masonry Wall-to-Timber Elements Connections Strengthened with Injection Anchors. *Eng. Struct.* **2014**, *81*, 98–109. [CrossRef]
23. Riccadonna, D.; Giongo, I.; Schiro, G.; Rizzi, E.; Parisi, M.A. Experimental Shear Testing of Timber–Masonry Dry Connections for the Seismic Retrofit of Unreinforced Masonry Shear Walls. *Constr. Build. Mater.* **2019**, *211*, 52–72. [CrossRef]
24. Solarino, F.; Oliveira, D.V.; Giresini, L. Wall-to-Horizontal Diaphragm Connections in Historical Buildings: A State-of-the-Art Review. *Eng. Struct.* **2019**, *199*, 109559. [CrossRef]
25. Parisi, M.A.; Piazza, M. Seismic Strengthening and Seismic Improvement of Timber Structures. *Constr. Build. Mater.* **2015**, *97*, 55–66. [CrossRef]
26. Branco, J.M.; Kekeliak, M.; Lourenço, P.B. In-Plane Stiffness of Traditional Timber Floors Strengthened with CLT. *Eur. J. Wood Wood Prod.* **2015**, *73*, 313–323. [CrossRef]
27. Ceccotti, A. Composite Concrete–Timber Structures. *Prog. Struct. Eng. Mater.* **2002**, *4*, 264–275. [CrossRef]
28. Dias, A.M.P.G.; Schänzlin, J.; Dietsch, P. (Eds.) *Design of Timber–Concrete Composite Structures: A State-of-the-Art Report by COST Action FP1402/WG4*; Shaker Verlag: Aachen, Germany, 2018; ISBN 978-3-8440-6145-1. [CrossRef]
29. Stepinac, M.; Rajčić, V.; Barbalić, J. Effect of Long-Term Loading on Timber–Concrete Composite Systems. *Građevinar* **2015**, *67*, 235–246. (In Croatian) [CrossRef]
30. Yeoh, D.; Fragiacomo, M.; De Franceschi, M.; Boon, K.H. State of the Art on Timber–Concrete Composite Structures: Literature Review. *J. Struct. Eng.* **2011**, *137*, 1085–1095. [CrossRef]
31. Lukaszewska, E.; Johnsson, H.; Fragiacomo, M. Performance of Connections for Prefabricated Timber–Concrete Composite Floors. *Mater. Struct.* **2008**, *41*, 1533–1550. [CrossRef]

32. Senaldi, I.; Magenes, G.; Penna, A.; Galasco, A.; Rota, M. The Effect of Stiffened Floor and Roof Diaphragms on the Experimental Seismic Response of a Full-Scale Unreinforced Stone Masonry Building. *J. Earthq. Eng.* **2014**, *18*, 407–443. [CrossRef]
33. Republic of Croatia. *Act on the Reconstruction of Buildings Damaged by Earthquakes in the City of Zagreb and the Krapina-Zagorje, Zagreb, Sisak-Moslavina and Karlovac Counties; Official Gazette of the Republic of Croatia, No. 21/2023*; Narodne novine: Zagreb, Croatia, 2023. (In Croatian)
34. Ministry of Construction and Physical Planning, Republic of Croatia. *Technical Regulation for Building Structures, Official Gazette of the Republic of Croatia Nos. 17/2017, 75/2020 and 7/2022*; Narodne novine: Zagreb, Croatia, 2017. (In Croatian)
35. Stepinac, M.; Rajčić, V.; Barbalić, J. Inspection and Assessment of Existing Timber Structures. *Građevinar* **2017**, *69*, 861–873. (In Croatian) [CrossRef]
36. Dietsch, P.; Kreuzinger, H. Guideline on the Assessment of Timber Structures: Summary. *Eng. Struct.* **2011**, *33*, 2983–2986. [CrossRef]
37. Luechinger, P.; Fischer, J.; Chrysostomou, C.; Dieteren, G.; Landon, F.; Leivestad, S.; Malakatas, N.; Mancini, G.; Markova, J.; Matthews, S.; et al. *New European Technical Rules for the Assessment and Retrofitting of Existing Structures*; Dimova, S., Vieira, P., Luechinger, A., Denton, P., Eds.; EUR 27128 EN; Publications Office of the European Union: Luxembourg, 2015. [CrossRef]
38. Nocetti, M.; Aminti, G.; Vicario, M.; Brunetti, M. Mechanical Properties of Ancient Wood Structural Elements Assessed by Visual and Machine Strength Grading. *Constr. Build. Mater.* **2024**, *411*, 134418. [CrossRef]
39. Nowak, T.; Patalas, F.; Karolak, A. Estimating Mechanical Properties of Wood in Existing Structures—Selected Aspects. *Materials* **2021**, *14*, 1941. [CrossRef] [PubMed]
40. Loebjinski, M.; Rug, W.; Pasternak, H. The Influence of Improved Strength Grading In Situ on Modelling Timber Strength Properties. *Buildings* **2020**, *10*, 30. [CrossRef]
41. *EN 338:2016*; Structural Timber—Strength Classes. CEN: Brussels, Belgium, 2016.
42. Krolo, J.; Damjanović, D.; Duvnjak, I.; Frančić Smrkić, M.; Bartolac, M.; Košćak, J. Methods for Determining Mechanical Properties of Masonry. *Građevinar* **2021**, *73*, 127–140. (In Croatian) [CrossRef]
43. Ortega, J.H.; Stepinac, M.; Lulić, L.; Núñez, G.M.; Saloustros, S.; Aranha, C.; Greco, F. Correlation between Sonic Pulse Velocity and Flat-Jack Tests for Estimating the Elastic Properties of Unreinforced Brick Masonry: Case Studies from Croatia. *Case Stud. Constr. Mater.* **2023**, *19*, e02467. [CrossRef]
44. Stepinac, M.; Lulić, L.; Damjanović, D.; Duvnjak, I.; Bartolac, M.; Lourenço, P.B. Experimental Evaluation of Unreinforced Brick Masonry Mechanical Properties by the Flat-Jack Method—An Extensive Campaign in Croatia. *Int. J. Archit. Herit.* **2024**, *18*, 691–708. [CrossRef]
45. Lulić, L.; Stepinac, M.; Bartolac, M.; Lourenço, P.B. Review of the Flat-Jack Method and Lessons from an Extensive Post-Earthquake Research Campaign in Croatia. *Constr. Build. Mater.* **2023**, *384*, 131407. [CrossRef]
46. Milić, M.; Stepinac, M.; Lulić, L.; Ivanišević, N.; Matorić, I.; Čačić Šipoš, B.; Endo, Y. Assessment and Rehabilitation of Culturally Protected Prince Rudolf Infantry Barracks in Zagreb after a Major Earthquake. *Buildings* **2021**, *11*, 508. [CrossRef]
47. *EN 14080:2013*; Timber Structures—Glued Laminated Timber and Glued Solid Timber—Requirements. CEN: Brussels, Belgium, 2013.
48. Ministero delle Infrastrutture e dei Trasporti. *Circolare 21 gennaio 2019, n. 7 C.S.LL.PP. Istruzioni per l'applicazione dell'«Aggiornamento delle "Norme tecniche per le costruzioni"» di cui al decreto ministeriale 17 gennaio 2018*; Gazzetta Ufficiale della Repubblica Italiana n. 35 del 11 febbraio 2019, Suppl. Ord. n. 5; Istituto Poligrafico e Zecca dello Stato: Rome, Italy, 2019. Table C8.5.I. (In Italian)
49. STA DATA. 3Muri—Software for the Seismic Analysis of Masonry Structures. Available online: https://www.stadata.com/en/3-muri-project/ (accessed on 31 July 2026).
50. Lagomarsino, S.; Penna, A.; Galasco, A.; Cattari, S. TREMURI Program: An Equivalent Frame Model for the Nonlinear Seismic Analysis of Masonry Buildings. *Eng. Struct.* **2013**, *56*, 1787–1799. [CrossRef]
51. Quagliarini, E.; Maracchini, G.; Clementi, F. Uses and Limits of the Equivalent Frame Model on Existing Unreinforced Masonry Buildings for Assessing Their Seismic Risk: A Review. *J. Build. Eng.* **2017**, *10*, 166–182. [CrossRef]
52. Penna, A.; Lagomarsino, S.; Galasco, A. A Nonlinear Macroelement Model for the Seismic Analysis of Masonry Buildings. *Earthq. Eng. Struct. Dyn.* **2014**, *43*, 159–179. [CrossRef]
53. Fajfar, P. A Nonlinear Analysis Method for Performance-Based Seismic Design. *Earthq. Spectra* **2000**, *16*, 573–592. [CrossRef]
54. *EN 1998-1:2004+A1:2013*; Eurocode 8: Design of Structures for Earthquake Resistance—Part 1: General Rules, Seismic Actions and Rules for Buildings. CEN: Brussels, Belgium, 2013.

55. *EN 1998-3:2005*; Eurocode 8: Design of Structures for Earthquake Resistance—Part 3: Assessment and Retrofitting of Buildings. CEN: Brussels, Belgium, 2005.
56. *EN 1995-1-1:2004+A2:2014*; Eurocode 5: Design of Timber Structures—Part 1-1: General—Common Rules and Rules for Buildings. CEN: Brussels, Belgium, 2014.
57. *EN 1991-1-1:2002*; Eurocode 1: Actions on Structures—Part 1-1: General Actions—Densities, Self-Weight, Imposed Loads for Buildings. CEN: Brussels, Belgium, 2002.
58. *EN 12369-1:2001*; Wood-Based Panels—Characteristic Values for Structural Design—Part 1: OSB, Particleboards and Fibreboards. CEN: Brussels, Belgium, 2001.
59. ICOMOS. *Recommendations for the Analysis, Conservation and Structural Restoration of Architectural Heritage*; ICOMOS: Paris, France, 2003.
60. *EN 1991-1-6:2005*; Eurocode 1: Actions on Structures—Part 1-6: General Actions—Actions during Execution. CEN: Brussels, Belgium, 2005.

Disclaimer/Publisher's Note: The statements, opinions and data contained in all publications are solely those of the individual author(s) and contributor(s) and not of MDPI and/or the editor(s). MDPI and/or the editor(s) disclaim responsibility for any injury to people or property resulting from any ideas, methods, instructions or products referred to in the content.